NIH Public Access
Author Manuscript
Eur J Neurosci. Author manuscript; available in PMC 2010 May 1.

Published in final edited form as:
Eur J Neurosci. 2009 May ; 29(10): 1964–1978. doi:10.1111/j.1460-9568.2009.06751.x.

Molecular architecture of endocannabinoid signaling at nociceptive synapses mediating analgesia

Rita Nyilas[1], **Laura C. Gregg**[2], **Ken Mackie**[3], **Masahiko Watanabe**[4], **Andreas Zimmer**[5], **Andrea G. Hohmann**[2], and **István Katona**[1]

1 *Institute of Experimental Medicine, Hungarian Academy of Sciences, H-1083 Budapest, Hungary*

2 *Neuroscience and Behavior Program, Department of Psychology, University of Georgia, Athens, Georgia 30602-3013*

3 *Department of Psychological and Brain Sciences, Indiana University, Bloomington, Indiana 47405*

4 *Department of Anatomy, Hokkaido University School of Medicine, Sapporo 060-8638, Japan*

5 *Institute of Molecular Psychiatry, University of Bonn, 53105 Bonn, Germany*

Abstract

Endocannabinoids suppress pain by acting at spinal, supraspinal and peripheral levels. However, the underlying molecular basis of endocannabinoid signaling is largely unknown. The lipid messenger 2-arachidonoylglycerol (2-AG) is emerging as the predominant endocannabinoid involved in rapid synaptic responses throughout the brain. Upon exposure to an environmental stressor, 2-AG is mobilized in the lumbar spinal cord in temporal correlation with stress-induced antinociception. We, therefore, characterized the precise molecular architecture of 2-AG signaling and its involvement in nociception in the rodent spinal cord. Non-radioactive *in situ* hybridization revealed that dorsal horn neurons widely expressed the mRNA of diacylglycerol lipase-alpha (DGL-α), the synthesizing enzyme of 2-AG. Peroxidase-based immunocytochemistry demonstrated high levels of DGL-α protein and CB_1 cannabinoid receptor, a receptor for 2-AG, in the superficial dorsal horn, at the first site of modulation of the ascending pain pathway. High-resolution electron microscopy uncovered postsynaptic localization of DGL-α at nociceptive synapses formed by primary afferents and revealed presynaptic position of CB_1 on excitatory axon terminals. Furthermore, DGL-α in postsynaptic elements receiving nociceptive input co-localized with metabotropic glutamate receptor 5 ($mGluR_5$), whose activation induces 2-AG biosynthesis. Finally, intrathecal activation of $mGluR_5$ at the lumbar level evoked endocannabinoid-mediated stress-induced analgesia through the DGL–2-AG–CB_1-pathway. Taken together, these findings suggest a key role for 2-AG-mediated retrograde suppression of nociceptive transmission at the spinal level. The striking positioning of the molecular players of 2-AG synthesis and action at nociceptive excitatory synapses suggests that pharmacological manipulation of spinal 2-AG levels may be an efficacious way to regulate pain sensation.

Keywords

DAGL; 2-AG; CB_1; metabotropic glutamate receptor; rodent spinal cord

Corresponding author: István Katona, PhD, Address: Institute of Experimental Medicine, Hungarian Academy of Sciences Szigony u. 43., H-1083 Budapest, Hungary, Phone: 36-1-2109400/195; Fax: 36-1-2109412, e-mail: E-mail: katona@koki.hu.

NIH-PA Author Manuscript
NIH-PA Author Manuscript
NIH-PA Author Manuscript

NIH-PA Author Manuscript

NIH-PA Author Manuscript

NIH-PA Author Manuscript

Introduction

Cannabis sativa has been used to alleviate pain since antiquity. Its analgesic effects can be attributed to its bioactive compounds, the cannabinoids (for review, see Di Marzo & Petrocellis, 2006). Cannabinoids such as Δ^9-tetrahydrocannabinol, the psychoactive ingredient in cannabis, produce antinociception both in animal models of acute and persistent pain and in clinical studies (for reviews, see Walker & Hohmann, 2005; Pacher *et al.*, 2006; Kogan & Mechoulam, 2007) by activation of CB_1 and CB_2 cannabinoid receptors (Ledent *et al.*, 1999; Zimmer *et al.*, 1999, Racz *et al.*, 2008; for reviews, see Pertwee, 2001; Guindon & Hohmann, 2008).

Cannabinoid receptors are physiologically activated by their endogenous ligands, the endocannabinoids (Piomelli, 2003). 2-arachidonoylglycerol (2-AG) (Mechoulam *et al.*, 1995; Sugiura *et al.*, 1995), a postulated ligand for both CB_1 and CB_2 (Sugiura *et al.*, 2006), is the predominant candidate endocannabinoid for being a fast synaptic messenger (Katona & Freund, 2008). A basic molecular organization scheme of 2-AG signaling in several brain areas is emerging (Katona *et al.*, 2006; Yoshida *et al.*, 2006; Lafourcade *et al.*, 2007; Uchigashima *et al.*, 2007; Matyas *et al.*, 2008) with postsynaptic positioning of diacylglycerol lipase-α (DGL-α) (Katona *et al.*, 2006; Yoshida *et al.*, 2006), the primary biosynthetic enzyme of 2-AG (Bisogno *et al.*, 2003), and presynaptic localization of CB_1 (Katona *et al.*, 1999; 2006; Kawamura *et al.*, 2006). Electrophysiological studies also suggest a retrograde action of 2-AG (Melis *et al.*, 2004; Makara *et al.*, 2005; Hashimotodani *et al.*, 2007, 2008), which has been proposed to function as a synaptic circuit breaker at brain glutamatergic synapses (Katona & Freund, 2008).

Endogenous 2-AG has also been implicated as a major transmitter subserving endocannabinoid-mediated stress-induced analgesia (Hohmann *et al.*, 2005; Suplita *et al.*, 2006). 2-AG, but not anandamide, is mobilized in lumbar spinal cord following exposure to footshock stress (Suplita *et al.* 2006). Moreover, spinal 2-AG levels correlate highly with stress antinociception (Hohmann & Suplita, 2006; Suplita *et al.*, 2006). although descending modulation from the periaqueductal gray is likely to play a predominant role. Finally, intrathecal administration of a pharmacological inhibitor of the 2-AG hydrolyzing enzyme monacylglycerol lipase markedly enhances stress antinociception in a CB_1-dependent manner (Suplita *et al.*, 2006). Despite 2-AG's widespread distribution and critical role in physiological pain regulation, the molecular machinery responsible for its spinal release and its involvement in pain sensation has not been identified. Previous studies reported that CB_1 receptors are expressed by primary sensory neurons including nociceptors (Hohmann & Herkenham, 1998; 1999; Ahluwalia *et al.*, 2000; Salio *et al.*, 2002; Mitrirattanakul *et al.*, 2006; Agarwal *et al.*, 2007), and CB_1 activation by cannabinoids inhibited C-fiber-mediated facilitation of spinal nociceptive responses (Strangman & Walker, 1999; Chapman, 1999; Drew *et al.*, 2000; Kelly & Chapman, 2001). However, the anatomical source of endogenous CB_1 ligands modulating nociceptive transmission is unknown.

In the present study, we describe the molecular architecture of 2-AG synthesis at primary nociceptive synapses and sites of 2-AG action in the rodent spinal cord using specific and highly sensitive antibodies and high-resolution electron microscopy. Behavioral studies combined with pharmacological manipulation of 2-AG signaling at the spinal level suggest the functional importance of this circuitry *in vivo*. These studies provide the first anatomical and functional evidence for the role of retrograde 2-AG signaling in nociception.

NIH-PA Author Manuscript

NIH-PA Author Manuscript

NIH-PA Author Manuscript

Materials and Methods

Perfusion and preparation of tissue sections

Experiments were carried out according to institutional guidelines of ethical code and the Hungarian Act of Animal Care and Experimentation (1998. XXVIII. Section 243/1998), which are in accordance with the European Communities Council Directive of November 24, 1986 (86/609/EEC). Adult wild type (n = 15, 186±131 days old) and CB_1 knockout (Zimmer *et al.*, 1999) (n = 3, 67 ± 9 days old) C57BL/6 mice and male Wistar rats (n = 2, 47 and 74 days old) were deeply anaesthetized with a mixture of ketamine-xylazine (25 mg/ml ketamine, 5 mg/ml xylazine, 0.1 w/w% promethazine in H_2O; 1 ml/100 g i.p.), then perfused with fixative containing 4% paraformaldehyde (PFA) in 0.1 M phosphate buffer (PB, pH: 7.4). Animals were perfused transcardially, first with 0.9% saline for 2 minutes, followed by either 100 ml or 400 ml (for mice or rats, respectively) of PFA fixative for 20 min. After perfusion, the spinal cord was removed from the spinal column and post-fixed for 2 hours in 4% PFA, and washed in 0.1 M PB. Transverse sections (50 μm thick) of the spinal cord at the cervical and lumbar levels were cut with a Leica VTS-1000 vibratome (Vibratome, St. Louis, MO, USA). For sections subjected to *in situ* hybridization, diethylpyrocarbonate (DEPC)-treated PB was used and sectioning was performed under RNase-free conditions. All reagents were purchased from Sigma-Aldrich, Merck, Roche (Basel, Switzerland) and Reanal (Budapest, Hungary), unless otherwise stated.

In situ hybridization

All solutions used for *in situ* hybridization were first treated with 0.1% DEPC and then autoclaved. Incubation of the slices was carried out in a free-floating manner in RNase-free sterile culture wells for all steps. After washing steps in phosphate-buffered saline containing 0.1% Tween-20 (PBST, pH 7.4), hybridization was performed at 60°C overnight in hybridization buffer containing the digoxigenin-labeled riboprobe (2.5 μg/ml) on a shaker in a humid chamber. We prepared digoxigenin-labeled antisense and sense riboprobes against the same region of the mouse DGL-α sequence that was previously used to characterize the regional and cellular expression pattern of DGL-α in the hippocampus (referred to as Probe 2 in Katona *et al.*, 2006). The length and the sequence of primers used for generating Probe 2 from cDNA derived from total C57BL/6 mouse frontal cortex mRNA are listed below the probe; numbering of the nucleotide positions starts from the beginning of the open reading frame: 1169 bp from 1967 to 3135 (forward primer: 5′-TCA TGG AGG GGC TCA ATA AG, reverse primer: 5′-CTA GCG TGC CGA GAT GAC CA). After incubation with either of the riboprobes, spinal cord sections from adult C57BL/6 wild-type mice (4 male, 105±23 days old; 1 female, 235 days old) were washed for 30 min at 60°C in wash solution 1 (containing 50% formamide, 5x SSC, and 1% SDS in DEPC-treated H_2O) and then twice for 45 min at 60°C in wash solution 2 (containing 50% formamide and 2x SSC in DEPC-treated H_2O) and in 0.05 M Tris-buffered saline containing 0.1% Tween-20 (TBST, pH 7.6), before sections were blocked in TBST containing 10% normal goat serum (TBSTN) for 1 hour at room temperature. Next, sections were incubated at 4°C overnight with sheep anti-digoxigenin Fab fragment conjugated to alkaline phosphatase (Roche Molecular Diagnostics, Germany) diluted at 1:1000 in TBSTN. The next day, after washing steps in TBST, sections were developed with the chromogen solution containing 5-bromo-4-chloro-3-indolyl-phosphate and Nitro blue tetrazolium chloride (3.5 μl/10 ml of both). The sections were rinsed in the developing solution in the dark for 6–18 hours, then the reaction was stopped using PBST and washed in PB. Sections were mounted in Vectashield (Vector Laboratories, Burlingame, CA, USA) onto glass slides and the coverslips were sealed with nail polish.

NIH-PA Author Manuscript

NIH-PA Author Manuscript

NIH-PA Author Manuscript

Peroxidase-based immunocytochemistry and pre-embedding immunogold labeling for electron microscopic analysis

After extensive washing in 0.1 M PB, spinal cord sections from adult C57BL/6 wild-type (10 male, 186±131 days old; 3 female, 55, 75 and 235 days old) and CB_1 knockout (Zimmer *et al.*, 1999) (2 male, 58 and 71 days old; 1 female, 76 days old) mice and Wistar rats (2 male, 47 and 74 days old) were first incubated for peroxidase-based immunocytochemistry for 10 min in 1% H_2O_2 in 0.1 M PB to block endogenous peroxidase activity, then washed in 0.1 M PB. Sections both for peroxidase-based immunocytochemistry and pre-embedding immunogold labeling were incubated in 30% sucrose overnight, followed by freeze-thawing over liquid nitrogen four times. After washing in 0.1 M PB, sections were processed either for immunoperoxidase, pre-embedding immunogold, pre-embedding immunogold combined with a second immunoperoxidase, or immunoperoxidase followed by pre-embedding immunogold staining. Subsequently, all washing steps and dilutions of the antibodies were done in 0.05 M Tris-buffered saline (TBS, pH 7.4). Following extensive washing in TBS, sections were blocked in 5% normal goat serum for 45 min, then incubated with one of the two polyclonal affinity-purified guinea pig anti-CB_1 (1:150–1:200 and 1:530; ~1 μg/ml) antibodies (Fukudome *et al.*, 2004) or with a polyclonal affinity-purified guinea pig or rabbit anti-DGL-α antibody (1:500, 0.76 μg/ml, termed 'C-42' in Yoshida *et al.*, 2006 or 1:1000–1:3000, ~0.3–1 μg/ml, termed 'INT' in Katona *et al.*, 2006, respectively) alone or mixed with an affinity-purified guinea pig anti-$mGluR_5$ antibody (1:300; ~1 μg/ml; Uchigashima *et al.*, 2007) for 48 hours at 4°C. To test the specificity of the DGL-α antibody, parallel staining on the neighboring sections from the same spinal cord was carried out with the mix of the DGL-α antibody and its blocking peptide (1 μg/ml) following their pre-incubation at 4°C overnight. The specificity of the anti-CB_1 antibodies was confirmed by the lack of immunostaining in sections derived from CB_1 knockout mice. In the immunoperoxidase staining procedure, after primary antibody incubations and TBS washing steps, sections were treated with biotinylated goat anti-guinea pig IgG or with biotinylated goat anti-rabbit IgG (both 1:300–1:500; Vector Laboratories, Burlingame, CA, USA), for 2 hours and then, after washing with TBS, incubated with avidin biotinylated-horseradish peroxidase complex (1:500; Elite-ABC, Vector Laboratories, Burlingame, CA, USA) for 1.5 hour. The immunoperoxidase reaction was developed, after washing with TBS and TB, using 3,3′-diaminobenzidine (DAB) as chromogen and 0.01% H_2O_2 dissolved in Tris buffer (TB, pH 7.6). In the immunogold staining procedure, sections were incubated in 0.8 nm gold-conjugated goat anti-guinea pig or goat anti-rabbit antibody for CB_1 and $mGluR_5$ or DGL-α, respectively (both 1:50; AURION, The Netherlands), overnight at 4°C. Then sections were silver intensified using the silver enhancement system R-GENT SE-EM according to the kit protocol (AURION, The Netherlands). In the double immunostaining experiments, sections were either developed first for immunogold and then for immunoperoxidase staining or first for immunoperoxidase and then for immunogold labeling. Lack of cross-reactivity of the secondary antibodies in the sequential detection scheme was verified by omission of the primary antibody, which eliminated labeling by the irrelevant secondary antibody. After development of the immunostaining, sections were treated with 0.5–1% OsO_4 in 0.1 M PB for 15–20 min, dehydrated in an ascending series of ethanol and acetonitrile, and embedded in Durcupan (ACM, Fluka, Buchs, Switzerland). During dehydration, sections were treated with 1% uranyl acetate in 70% ethanol for 15–20 min. From sections embedded in Durcupan, areas of interest were re-embedded and re-sectioned for electron microscopy. Ultrathin sections (60 nm thickness) were collected on Formvar-coated single-slot grids and stained with lead citrate.

Light and electron microscopic analysis and image processing

Tissue sections subjected to *in situ* hybridization and peroxidase-based immunocytochemistry were analyzed on a ZEISS Axioplan 2 microscope using Plan-NEOFLUAR 5x – 63x objectives and were photographed with an Olympus DP70 digital camera. Electron micrographs were

NIH-PA Author Manuscript

NIH-PA Author Manuscript

NIH-PA Author Manuscript

taken at 30,000 – 50,000x magnification with a Hitachi 7100 electron microscope. For the adjustment of digital photographs, Adobe Photoshop CS2 software (Adobe Systems, San Jose, CA, USA) was used. In all imaging processes, adjustments (brightness and contrast) were adjusted in the whole frame and no part of an image was modified separately in any way.

Ultrastructural criteria for nociceptive axon terminal identification

For the identification of nociceptive axon terminals in the spinal dorsal horn, we used the following morphological criteria defining synaptic glomeruli described previously (Ribeiro-da-Silva & Coimbra, 1982; Ribeiro-da-Silva, 1995). Type I glomeruli formed by unmyelinated (mainly nociceptive C-) fibers occurring predominantly in dorsal lamina II (LII outer - dorsal LII inner), were identified by bearing a small central terminal of indented contour with dark axoplasm, closely packed clear spherical vesicles of variable size and only very few mitochondria. A subpopulation of these terminals containing more than three dense core vesicles corresponds to peptidergic unmyelinated fibers. Around the core terminal, dendritic spines, vesicle containing dendritic spines and axon endings were situated. Type II glomerular terminals of small myelinated primary afferents (Aδ-fibers) prevailed in ventral lamina II (ventral LII inner) and lamina III, were identified as electron-lucent, large boutons with regular contour and loosely distributed, agranular round synaptic vesicles of uniform diameter, numerous mitochondria and sometimes neurofilaments, surrounded by fewer vesicle-containing dendrites and more axon endings. In apposition to the core bouton of a glomerulus at least four surrounding profiles and two or more synaptic specializations were required to become accepted as a type I or type II glomerulus. To determine whether the terminals fulfill these criteria, they were followed through consecutive serial sections.

Surgical procedures

One hundred and fifty four adult male Sprague-Dawley rats were used in the *in vivo* experiments. All procedures were approved by the University of Georgia Animal Care and Use Committee and followed the guidelines for the treatment of animals of the International Association for the Study of Pain (Zimmermann, 1983).

Rats were anesthetized using a sodium pentobarbital and ketamine mixture (25 mg/kg and 40 mg/kg, respectively), administered intraperitoneally. PE10 tubing was used to construct the intrathecal catheters (Yaksh & Rudy, 1976; Hohmann *et al.* 1998). Catheters were implanted through an incision in the atlanto-occipital membrane to a depth of 8.5 cm so that the catheter tip was positioned rostral to the lumbar enlargement. Catheters were anchored to the skull with dental acrylic and a stainless steel screw. Animals exhibiting signs of motor dysfunction induced by intrathecal catheter placement were discarded and did not receive pharmacological manipulations. Animals were allowed to recover five to seven days prior to testing.

Drug preparation and administration

(*S*)-3,5-dihydroxyphenylglycine (DHPG) was obtained from Tocris Cookson (Ellisville, MO, USA). *N*-(piperidin-1-yl)-5-(4-chlorophenyl)-1-(2,4-dichlorophenyl)-4-methyl-1H-pyrazole-3-carboxamide (SR141716A, rimonabant) was a gift from NIDA. *N*-formyl-L-leucine (1S)-1-[[(2S,3S)-3-hexyl-4-oxo-2-oxetanyl]methyl]dodecyl ester ((−)-tetrahydrolipstatin, THL) and 2-methyl-6-(phenylethynyl)pyridine hydrochloride (MPEP hydrochloride) were obtained from Sigma-Aldrich (St. Louis, MO, USA). All drugs were dissolved in a vehicle containing 60% DMSO and 40% saline. Drugs were delivered in a single 10 μl volume and delivered intrathecally (i.t.). Therefore, for all experiments requiring co-administration of multiple agents, all compounds were administered intrathecally (i.t.) in a single 10 μl volume of 60% DMSO: 40% saline. Vehicle groups, therefore, always consisted of a single 10 μl injection of 60% DMSO: 40% saline. Effects of pharmacological manipulations were always compared to controls employing the same 60% DMSO-containing

NIH-PA Author Manuscript

NIH-PA Author Manuscript

NIH-PA Author Manuscript

vehicle tested under identical conditions by a single experimenter, blinded to the drug condition.

Behavioral testing

Stress antinociception was quantified behaviorally using the tail-flick test (D'Amour, 1941), which measures the latency for a rat to remove its tail from a radiant heat source (IITC Inc., Model 33A, Woodland Hills, CA, USA). Rats were habituated to the restraining tubes for 15 min prior to testing. Cut-off latencies (10 or 15 sec) were uniformly employed within any given study to prevent tissue damage. The 15 sec cutoff latency was employed to facilitate detection of enhancements in stress antinociception induced by pharmacological manipulations. Stable baseline withdrawal responses to thermal stimulation of the tail were initially established prior to pharmacological manipulations. Intrathecal injections were administered manually using a Hamilton syringe and consisted of 10 μl of drug or vehicle followed by 10 μl of saline to flush the catheter. Immediately following injection, tail-flick latencies were measured three times at 2 min intervals and averaged to assess possible changes in nociceptive thresholds induced by pharmacological manipulations before exposure to footshock stress. Rats were subsequently exposed to continuous footshock for 3 min (0.9 mA, AC current) to induce stress antinociception, as described previously (Hohmann *et al.*, 2005; Suplita *et al.* 2005, 2006, 2008). Tail-flick latencies were measured over 40 min following footshock at 2 min intervals. Every two consecutive measurements were averaged for each rat before (baseline) and after (post shock) exposure to footshock to create two point blocks that were used for repeated measure statistical analyses, using methods identical to those reported previously (Hohmann *et al.*, 2005; Suplita *et al.* 2005, 2006, 2008). Group means of these two point averages are depicted graphically in Fig. 6 and Fig. 7. Intrathecal injections were delivered 5 min prior to exposure to footshock. Catheter placements were verified following completion of testing by injection of fast green dye followed by dissection. Animals exhibiting damage to the spinal cord induced by catheter placement were excluded from data analysis. In all experiments, the experimenter was blinded to the experimental condition.

Role of group I metabotropic glutamate receptors in endocannabinoid-mediated stress antinociception

To determine whether activation of group I mGluRs in the spinal cord altered endocannabinoid-mediated stress antinociception, rats received either the group I mGluR agonist DHPG (0.02 or 0.2 μg i.t.) or vehicle intrathecally prior to exposure to footshock. Separate groups received the group I $mGluR_5$ antagonist MPEP (2.3×10^{-5}, 2.3×10^{-4} and 0.23 μg i.t.) or vehicle to determine whether blockade of $mGluR_5$ receptors at the spinal level would suppress stress antinociception. Low doses of DHPG and MPEP were selected to avoid alterations in basal nociceptive thresholds in the tail-flick test (Gabra *et al.* 2007), which was also confirmed in the present experiments. To determine pharmacological specificity, separate groups received either DHPG (0.2 μg i.t.), DHPG (0.2 μg i.t.) co-administered with MPEP (2.3×10^{-5} μg i.t.), or vehicle prior to exposure to the stressor. To determine whether DHPG-induced changes were dependent upon CB_1 receptor activation, DHPG (0.2 μg i.t.) was administered alone or co-administered with rimonabant (10 μg i.t.). The dose of rimonabant was selected based upon our previous work documenting that intrathecal administration of the same dose was insufficient to inhibit stress antinociception (Suplita *et al.*, 2006). Tail-flick latencies were measured before and after exposure to footshock as previously described (Hohmann *et al.*, 2005; Suplita *et al.*, 2006).

Role of DGL in endocannabinoid-mediated stress antinociception

To determine whether pharmacological inhibition of DGL at the spinal level suppressed endocannabinoid-mediated stress antinociception, rats received either THL (10 or 100 μg i.t),

NIH-PA Author Manuscript

NIH-PA Author Manuscript

NIH-PA Author Manuscript

at doses that lacked intrinsic effects on basal nociceptive thresholds in the absence of footshock, or vehicle intrathecally. Effects of a low dose of THL (1 μg i.t.) on stress antinociception was additionally compared to vehicle using the same cutoff latency (15 sec) employed to facilitate detection of enhancements of stress antinociception induced by intrathecal DHPG. To evaluate whether activation of group I mGluRs at the spinal level enhanced stress antinociception through a DGL-dependent mechanism, DHPG (0.2 μg i.t.) was administered either alone or co-administered with THL (1 μg i.t.). Tail-flick latencies were measured before and after exposure to footshock as previously described (Hohmann *et al.*, 2005; Suplita *et al.*, 2006).

Statistical analysis

Behavioral data were analyzed by repeated measures Analysis of Variance (ANOVA) and ANOVA using methods identical to those employed in our previously published work (Hohmann et al. 2005; Suplita et al., 2005, 2006, 2008). SPSS (version 16.0, SPSS Incorporated, Chicago, IL, USA) statistical software was employed for all analyses. For each animal, every two consecutive tail-flick latencies was averaged before (baseline) and after (post-shock) latencies. Means of these two point blocks were used in the repeated measures ANOVA. Baseline and post shock tail-flick latencies were analyzed separately with drug treatment serving as the between subjects factor and time serving as the within subjects factor. Post-injection tail-flick latencies, determined immediately prior to footshock exposure, were averaged into a single determination for each animal, and averaged across animals for each drug treatment; this measure was calculated to facilitate statistical comparisons of drug-induced changes in the basal nociceptive threshold observed prior to footshock (post-injection tail-flick latency), with baseline tail-flick latencies. In all studies, the Greenhouse-Geisser (1959) correction was applied to the interaction term of all repeated factors. *Post hoc* comparisons were evaluated for all main effects using Fisher's Protected Least-Squares Difference (LSD) to correct for inflated alpha error, with $P < 0.05$ considered as statistically significant.

Results

Distribution of DGL-α enzyme and CB_1 receptor in the spinal cord

To determine the cellular source of 2-AG in the spinal cord, we first examined the expression pattern of DGL-α, its main synthesizing enzyme (Bisogno *et al.*, 2003). Non-radioactive free-floating *in situ* hybridization on mouse spinal cord sections with an antisense riboprobe revealed widespread DGL-α expression throughout the spinal cord (Fig. 1A and C), whereas no significant labeling was found with the control sense probe (Fig. 1B). Most, if not all neurons expressed DGL-α mRNA at variable levels in the dorsal horn (Fig. 1C and D), but DGL-α positive cells were also scattered in the intermediate spinal cord (Fig. 1A). Remarkably, the highest DGL-α mRNA expression in the spinal cord was observed in large cells presumably corresponding to the spinal motoneurons in the ventral horn (Fig. 1A). Importantly, we must note that the *in situ* hybridization reactionswere performed under highly stringent conditions to avoid any nonspecific labeling, which may have resulted in reduced sensitivity. Nevertheless, the widespread distribution of DGL-α mRNA suggests that spinal cord neurons in all spinal laminae express the synthesizing enzyme of 2-AG.

To elucidate the distribution of the DGL-α protein in the spinal cord, immunostainings for DGL-α with a DGL-α 'INT' rabbit antibody directed against a 118 residue long internal segment of the enzyme (residues 790-908) and with a C-42 guinea pig antibody raised against the C-terminal tail (residues 1003-1044) were carried out on wild-type mouse and rat spinal cord sections (Fig. 2A–D and I; Suppl. Fig. 1A). A widespread punctate immunolabeling pattern was found with both antibodies directed against independent epitopes across the entire grey matter, with the highest density located in the dorsal horn of the spinal cord, the central termination zone of primary afferents (Fig. 2A,C and I; Suppl. Fig. 1A). Besides the

NIH-PA Author Manuscript

NIH-PA Author Manuscript

NIH-PA Author Manuscript

characteristic punctate labeling, scattered cell bodies immunoreactive for DGL-α were also visualized by the staining in the ventral spinal cord (Fig. 2A). When the peptide fragment used as epitope for antibody generation was added to the primary antibody incubation mixture no labeling was found on spinal cord sections (Fig. 2B and D).

Light microscopic analysis of CB_1 immunostaining performed by a highly sensitive antibody (Fukudome *et al.*, 2004) revealed a very similar distribution of the CB_1 receptor to that of DGL-α in the mouse and rat dorsal spinal cord (Fig. 2E,G and J; Suppl. Fig. 1B). The most profound CB_1-immunoreactivity was seen in the superficial layers, where strong accumulation of the receptor protein was represented by very dense puncta at higher magnification (Fig. 2J). Strong staining was also observed in the dorsolateral funiculus, where longitudinal fibers of intrasegmental connections, ascending projections and descending modulatory systems are situated (Fig. 2E and G; Suppl. Fig. 1B), and also in lamina X, around the central canal, in a site of termination of visceral afferents (Fig 2E). Interestingly, a dense CB_1 staining was also seen in the ventral horn, in the same area where strong DGL-α immunoreactivity was observed (Fig. 2E, 2A). The specificity of the antibody was confirmed by the lack of immunolabeling in sections derived from CB_1 knockout mice (Fig. 2F,H). Taken together, immunostaining for DGL-α and CB_1 provide evidence that the molecular components responsible for mediating 2-AG synthesis and action are present in the spinal cord with the highest density in the termination zone of primary nociceptive axons.

Postsynaptic DGL-α enzyme and presynaptic CB_1 receptor are located at primary nociceptive synapses

To determine which subcellular compartments underlie the characteristic punctate staining pattern observed at the light microscopic level, we performed a detailed electron microscopic analysis of DGL-α localization in mouse and rat spinal cord sections. Samples for electron microscopy were selected from layers I-III of the dorsal spinal cord to ensure complete primary afferent distribution in the superficial layers. High-magnification electron microscopic analysis demonstrated that the diffusible DAB end product of the immunoperoxidase staining, which indicates the subcellular localization of DGL-α, was concentrated in a large number of dendritic spine heads (Fig. 3A, C; Suppl. Fig. 1C) and also in small diameter dendrites (Fig. 3D; Suppl. Fig. 1D). The DGL-α-immunopositive spines and dendrites received asymmetric synapses from DGL-α-negative excitatory axon terminals (Fig. 3A), including boutons belonging to either type I or type II synaptic glomeruli based on their morphological features (Ribeiro-da-Silva & Coimbra, 1982; for detailed ultrastructural criteria, see Methods) and corresponding to nerve endings of unmyelinated C- (Fig. 3C; Suppl. Fig. 1C) or myelinated Aδ-fibers (Fig. 3D; Suppl. Fig. 1D), respectively. In contrast to the high densitiy of DGL-α at asymmetric synapses, the presence of this enzyme at symmetric, putative glycinergic and/or GABAergic synapses could not be unequivocally established. However, we cannot rule out the possibility that DGL-α is also present at inhibitory synapses at low levels. False negative results in our immunostainings could be due to several factors such as epitope masking at inhibitory synapses and/or insufficient affinity of the antibodies and our labeling method to visualize the enzyme at very low density (Fritschy, 2008).

Silver-intensified immunogold staining also confirmed the subcellular accumulation of DGL-α on spine heads and dendrites situated postsynaptically to small excitatory axon terminals and both types of synaptic glomeruli in the superficial dorsal horn (Fig. 3B,E,F). The gold particles representing the precise position of the transmembrane protein DGL-α were always observed on the plasma membrane of second order spinal neurons that received glutamatergic synaptic contact from either C- (Fig. 3E) or Aδ-fibers (Fig. 3F). Furthermore, DGL-α was often found next to the postsynaptic density of excitatory synapses in a characteristic perisynaptic position (Fig. 3B,E,F).

NIH-PA Author Manuscript

NIH-PA Author Manuscript

NIH-PA Author Manuscript

In the next set of experiments, we aimed to unravel whether there is an anatomical basis of group I metabotropic glutamate receptor (mGluR)–induced 2-AG synthesis in the dorsal spinal cord, as previously described in several brain areas (Robbe *et al.*, 2002; Jung *et al.*, 2005, 2007; Lafourcade *et al.*, 2007; Uchigashima *et al.*, 2007; Drew *et al.*, 2008). In co-localization experiments, we performed double immunogold–immunoperoxidase (DAB) immunostainings using anti-DGL-α antibody developed in rabbit and anti-$mGluR_5$ developed in guinea pig. Extensive electron microscopic analysis confirmed that DGL-α was indeed localized on $mGluR_5$-positive dendritic spines receiving asymmetrical synapses from central axon terminals of C- and Aδ-fibers (type I or II synaptic glomeruli, respectively) (Fig. $4A_1$–B). These anatomical findings demonstrate that the enzymatic machinery of 2-AG synthesis and its upstream triggering receptor are located around the postsynaptic side of primary nociceptive synapses.

Cellular and ultrastructural localization of CB_1 cannabinoid receptor in the spinal cord have been controversial to date (Hohmann & Herkenham, 1998; Farquhar-Smith *et al.*, 2000; Salio *et al.*, 2002; Agarwal *et al.*, 2007). To determine the precise subcellular distribution of 2-AG's molecular target, we used a highly sensitive second generation CB_1 antibody whose specificity has been confirmed in CB_1 knockout animals (Fig. 2E,F) (Fukudome *et al.*, 2004). Electron microscopic analysis in the superficial dorsal horn of mouse and rat spinal cords revealed that the diffusible reaction product DAB, indicating the presence of CB_1 receptor, was concentrated predominantly in excitatory axon terminals, forming asymmetrical synapses (Fig. 5A,B; Suppl. Fig. 1E $_1$–F). Moreover, presynaptic CB_1 immunolabeling was also found, albeit at a low degree, in axon endings that can be identified by morphological criteria as forming type I or type II synaptic glomeruli (Ribeiro-da-Silva & Coimbra, 1982) (Fig. 5E,F; Suppl. Fig. 1F,G). In accordance, immunogold staining also confirmed presynaptic CB_1 receptors on small boutons (Fig. 5C,D) and on primary nociceptive axon terminals (Fig. 5G,H) both forming asymmetrical synapses on their postsynaptic targets. Gold particles, indicating the precise subcellular position of CB_1, were always attached to the presynaptic plasma membrane, often adjacent to the active zone (Fig. 5C,G,H).

Retrograde 2-AG signaling mediates $mGluR_5$-dependent analgesia in vivo

The above anatomical findings indicate that the molecular machinery initiating retrograde 2-AG signaling is present at nociceptive synapses. Thus, in subsequent experiments, we examined functional evidence for the involvement of this molecular machinery in endocannabinoid-mediated stress-induced analgesia (SIA), a behavioral phenomenon in which animals are less responsive to noxious stimulation following exposure to an environmental stressor. This animal model of stress-induced analgesia (Hohmann *et al.*, 2005) was previously demonstrated to mobilize 2-AG, but not anandamide, in the lumbar spinal cord (Suplita *et al.*, 2006). Baseline tail-flick latencies, measured prior to drug or vehicle administration, did not differ between groups with one exception. In each study, vehicle alone had no effect on the basal nociceptive threshold, assessed relative to baseline tail-flick latencies. Moreover, none of the drugs, some of which were specifically employed at low doses, altered the basal nociceptive threshold; post-injection tail-flick latencies, assessed prior to footshock, did not differ between groups in any study. Thus, the pharmacological manipulations employed here specifically altered tail-flick latencies in a state dependent fashion that was apparent under conditions in which the endocannabinoid system was specifically activated during stress antinociception. In all studies, exposure to footshock stress produced antinociception, as revealed by the observation of time-dependent changes in post-shock tail-flick latencies (main effect of post-shock time: $P < 0.0001$).

Intrathecal administration of the group I mGluR agonist DHPG (0.02 or 0.2 μg i.t.) induced a time-dependent enhancement of post-shock tail-flick latencies relative to vehicle controls

NIH-PA Author Manuscript

NIH-PA Author Manuscript

NIH-PA Author Manuscript

(interaction between DHPG and post-shock time: $F_{18,225} = 2.14$, $P = 0.02$; Fig. 6A). The $mGluR_5$ antagonist MPEP strongly suppressed the antinociceptive effect produced by footshock (main effect of MPEP: $F_{3,30} = 3.52$, $P = 0.03$; Fig. 6B) and altered the time course of stress antinociception (interaction between MPEP and post-shock time: $F_{27,270} = 4.63$, $P < 0.0001$; Fig. 6B). *Post hoc* analysis revealed that the high (0.23 μg i.t.) and middle doses (2.3×10^{-4} μg i.t.) of MPEP suppressed stress antinociception relative to the low (2.3×10^{-5} μg i.t.) dose ($P = 0.01$ and $P = 0.049$, respectively). The high dose of MPEP also suppressed stress antinociception relative to vehicle ($P = 0.02$). The low dose of MPEP was insufficient to alter stress antinociception ($P = 0.70$). This same dose of MPEP nonetheless blocked the time-dependent enhancement of stress antinociception induced by DHPG (0.2 μg i.t.) (interaction between drug treatment and post-shock time: $F_{18,207} = 2.81$, $P = 0.006$; Fig. 6C). Stress antinociception was greater in groups receiving DHPG (0.2 μg i.t.) alone compared to DHPG co-administered with MPEP (main effect of treatment: $F_{1,14} = 4.79$, $P = 0.046$). By contrast, stress antinociception was similar in groups receiving vehicle and groups receiving DHPG co-administered with MPEP ($F_{1,16} = 0.003$, $P = 0.96$). The CB_1 antagonist rimonabant (10 μg i.t.) also blocked the time-dependent enhancement of stress antinociception induced by DHPG (interaction between drug treatment and post shock time: $F_{18,225} = 2.29$, $P = 0.03$; Fig. 6D). Stress antinociception was greater in groups receiving DHPG (0.2 μg i.t.) alone compared to DHPG co-administered with rimonabant over 25 min post-shock (interaction between drug treatment and post-shock time: $F_{6,84} = 2.92$, $P = 0.04$; Fig. 6D). By contrast, stress antinociception was similar in groups receiving either vehicle or DHPG co-administered with rimonabant over the same interval ($F_{6,108} = 1.52$ $P = 0.20$). THL, the most potent pharmacological inhibitor of DGL (Bisogno *et al.*, 2003;2006) presently available, also suppressed stress antinociception relative to vehicle controls (main effect of THL: $F_{2,27} = 4.43$, $P = 0.02$; Fig. 7A). Both the high (100 μg i.t.; $P = 0.02$) and middle (10 μg i.t.; $P = 0.04$) doses of THL similarly suppressed post-shock tail-flick latencies relative to vehicle. The low dose of THL (1 μg i.t.) was insufficient to alter post-shock tail-flick latencies ($F_{1,12} = 0.64$, $P = 0.44$; Fig. 7B) but, nonetheless, blocked the DHPG-induced enhancement of stress antinociception (interaction between drug treatment and post-shock time: $F_{18,189} = 9.40$, $P < 0.0001$, Fig. 7C). Stress antinociception was greater (main effect of drug treatment: $F_{2,21} = 15.07$, $P < 0.0001$, Fig. 7C) in groups receiving DHPG (0.2 μg i.t.) compared to groups receiving either DHPG (0.2 μg i.t.) co-administered with THL (1 μg i.t.) or vehicle ($P < 0.0001$ for each comparison). Co-administration of DHPG together with THL did not alter stress antinociception relative to vehicle ($P = 0.91$, Fig. 7C). Taken together, these data show that the $mGluR_5$–DGL-α–CB_1 pathway mediates stress-induced analgesia.

Discussion

Various experimental approaches have been applied to characterize the antinociceptive effects of exogenous cannabinoids in acute and persistent pain states (for review, see Walker & Hohmann, 2005). However, the molecular architecture of endogenous cannabinoid signaling involved in the physiological regulation of pain transmission has remained largely unknown. Here, we provide anatomical evidence that $mGluR_5$ and DGL-α, the first and last molecular components in the biosynthetic pathway of the endocannabinoid 2-AG, are concentrated on the postsynaptic side of primary nociceptive synapses, while its effector, the CB_1 cannabinoid receptor is enriched presynaptically. Furthermore, we show that these molecular players are functionally linked together in the production of endocannabinoid-mediated stress-induced analgesia *in vivo*. These findings suggest that nociceptive synapses are equipped with an intrinsic feedback system, the retrograde 2-AG signaling pathway, which regulates nociception in an activity-dependent manner.

NIH-PA Author Manuscript

NIH-PA Author Manuscript

NIH-PA Author Manuscript

Molecular components of retrograde 2-AG signaling are present at central synapses of primary nociceptive afferents

The dorsal spinal cord has a pivotal role in nociceptive sensory information processing. Neurons in laminae I–III of Rexed receive most inputs from unmyelinated polymodal C- and thinly myelinated mechanoreceptor Aδ-fibers of primary afferents (for review, see Millan, 1999), the vast majority of which (approximately 90% of C-fibers and 70% of Aδ-fibers) carry nociceptive information (Fang *et al.*, 2005). A remarkable morphological feature of these afferents, classified physiologically on the basis of their conduction velocities, is their characteristic central axon terminal surrounded by other synaptic profiles, forming the so-called synaptic glomeruli (Ribeiro-da-Silva & Coimbra, 1982; Réthelyi *et al.*, 1982). Using specific morphological criteria of synaptic glomeruli (Ribeiro-da-Silva & Coimbra, 1982; Ribeiro-da-Silva, 1995; see Methods for details), we identified primary afferent terminals in the spinal dorsal horn and demonstrated the presence of molecular players of 2-AG synthesis and action at excitatory synapses formed by C- and Aδ-fibers.

Cellular and subcellular sources of endocannabinoids have not previously been identified in the spinal cord before. Our results show that DGL-α is accumulated in the superficial dorsal horn and located postsynaptically to primary afferents, providing a neuroanatomical basis for retrograde 2-AG signaling upon activation of primary nociceptors. DGL-α and its upstream activator, the group I metabotropic glutamate receptor $mGluR_5$, whose activation triggers 2-AG synthesis (Jung *et al.*, 2005), are both concentrated perisynaptically on dendritic spinesat central glutamatergic synapses (Lujan *et al.*, 1996; Katona *et al.*, 2006). This precise co-localization suggests that these proteins are functionally coupled at these synapses in the so-called perisynaptic signaling machinery (PSM) to detect excessive glutamate release and produce ‘on demand’ retrograde 2-AG signaling (Katona & Freund, 2008). In the spinal cord, ultrastructural analysis has demonstrated that $mGluR_5$ occurs postsynaptically to excitatory axon terminals, and it is located in dendrites receiving synapses from primary afferent Aδ- and C-glomerular fiber endings (Tao *et al.*, 2000; Alvarez *et al.*, 2000; Pitcher *et al.*, 2007). Here, we provide evidence for co-localization of DGL-α and $mGluR_5$ in postsynaptic compartments apposing these terminals. This demonstration proves that the molecular machinery for $mGluR_5$-induced 2-AG synthesis, as previously described in the brain (Uchigashima *et al.*, 2007; Lafourcade *et al.*, 2007), is also present on the postsynaptic side of nociceptive synapses formed by incoming primary afferents.

Our high-resolution anatomical analysis demonstrated that CB_1 receptors, the molecular targets of 2-AG, are located presynaptically, on small excitatory axon terminals and on primary afferent fiber endings. Several studies have reported widespread CB_1 distribution in the spinal cord (Farquhar-Smith *et al.*, 2000; Salio *et al.*, 2002; Hohmann & Herkenham, 1998; Hohmann *et al.* 1999), and PKCγ-immunoreactive excitatory interneurons were proposed as the predominant CB_1-positive cell type in the dorsal horn (Farquhar-Smith *et al.*, 2000). However, the presence of CB_1 on central primary afferent terminals has remained ambiguous because of modest CB_1 co-localization with primary afferent markers and minor reduction in CB_1-immunoreactivity after dorsal rhizotomy (Farquhar-Smith *et al.*, 2000; Price *et al.*, 2003; see also Ahluwalia *et al.*, 2000; Mitrirattanakul *et al.*, 2006; Agarwal *et al.*, 2007). Low antibody sensitivity may have contributed to this interpretation, because the high affinity cannabinoid agonist [^{3}H]CP55,940 binding demonstrated using quantitative autoradiography was reduced by approximately 50% after extensive unilateral dorsal rhizotomy (Hohmann *et al.*, 1999). Importantly, novel, highly sensitive second generation CB_1 antibodies that could detect CB_1 receptors on hippocampal glutamatergic axons (Kawamura *et al.*, 2006; Katona *et al.*, 2006), in which CB_1 protein levels were under detection threshold for antibodies previously used in spinal cord studies (Katona *et al.*, 1999; Egertova & Elphick, 2000; Farquhar-Smith *et al.*, 2000; Salio *et al.*, 2002), were employed here. Use of this second generation antibody has

NIH-PA Author Manuscript

NIH-PA Author Manuscript

NIH-PA Author Manuscript

enabled us to directly demonstrate the presence of CB_1, albeit at low levels, on central terminals of primary nociceptive C- and Aδ-fibers. CB_1 activation also inhibits C-fiber- and A-fiber-evoked neuronal responses of dorsal horn neurons (Chapman, 1999; Strangman & Walker, 1999; Drew *et al.*, 2000; Kelly & Chapman, 2001; Morisset & Urban, 2001). The physiological and anatomical findings together suggest that 2-AG, released from dendritic processes situated postsynaptically to primary afferent terminals, can target presynaptic CB_1 receptors, located either on nociceptive fibers or local excitatory interneurons, thereby leading to inhibition of nociceptive excitatory transmission.

Spinal 2-AG signaling is involved in group I mGluR-dependent stress-induced analgesia in vivo

In our behavioral experiments, we aimed to determine what functional roles the molecular components of 2-AG signaling, described at primary nociceptive synapses, may play in pain sensation *in vivo*, using an animal model of endocannabinoid-mediated stress-induced analgesia. Group I mGluRs have previously been implicated in modulating exogenous cannabinoid antinociception (Palazzo *et al.*, 2001). Here we show that activation of $mGluR_5$ enhances endogenous cannabinoid-mediated stress antinociception under physiological conditions, in a manner dependent upon DGL and CB_1 receptor activation. These results are in accordance with *in vitro* and *in vivo* electrophysiological, biochemical and anatomical studies suggesting a functional link between $mGluR_5$ and endocannabinoid signaling (Maejima *et al.*, 2001; Robbe *et al.*, 2002; de Novellis *et al.*, 2005; Lafourcade *et al.*, 2007; Drew *et al.*, 2008) in the brain.

Exposure to the footshock stressor used here to induce stress antinociception elevates 2-AG, but not anandamide, levels in the lumbar spinal cord (Suplita *et al.*, 2006). Moreover, stress antinociception correlates highly with 2-AG mobilization in the lumbar spinal cord (Suplita *et al.*, 2006) and cannot be attributed to motor suppression (Suplita *et al.*, 2008). The involvement of 2-AG in stress-antinociception at the spinal level is further supported by the observation that intrathecal inhibition of monoacylglycerol lipase, the major degrading enzyme of 2-AG (Dinh *et al.*, 2002; Blankman *et al.*, 2007), produces a profound CB_1-mediated enhancement of SIA (Suplita *et al.*, 2006). These findings are consistent with the *in vitro* results documenting that $mGluR_5$ activation induces 2-AG release (Jung *et al.*, 2005; 2007; Lafourcade *et al.*, 2007; Uchigashima *et al.*, 2007; Drew *et al.*, 2008), but does not alter ananadamide levels in brain slice cultures (Jung *et al.*, 2005). The observations that postsynaptic group I mGluRs activate phospholipase Cβ (PLCβ) (Pin & Duvoisin, 1995) and that 2-AG biosynthesis is initiated by activation of the PLCβ-DGL pathway *in vitro* (Bisogno *et al.*, 2003; Jung *et al.*, 2005; 2007; Hashimotodani *et al.*, 2008) suggest that $mGluR_5$ activation induces PLCβ-mediated diacylglycerol production that serves as a precursor for DGL-α-mediated 2-AG synthesis. Indeed, pharmacological inhibition of DGL at the spinal level with intrathecal THL suppressed endocannabinoid-mediated SIA in our study. The enhancement of stress antinociception induced by group I mGluR activation with DHPG was also blocked by a pharmacological inhibitor of DGL. Thus, DHPG enhanced stress antinociception only under conditions in which 2-AG is mobilized at the spinal level to produce endocannabinoid-mediated SIA (Suplita *et al.*, 2006).

We have previously demonstrated that spinal antagonism of CB_1 *per se* did not alter the phenomenon of footshock-induced non-opioid SIA, although spinal 2-AG levels were nonetheless selectively increased by the same footshock stressor and correlated highly with SIA (Suplita *et al.*, 2006). On the other hand, here we provide evidence that enhancement of SIA by group I mGluR activation requires activation of CB_1 as a necessary, but not sufficent, prerequisite at the spinal level. Because the CB_1 antagonist rimonabant microinjected into the dorsolateral PAG at the same dose strongly suppressed stress-antinociception *per se* (Hohmann

NIH-PA Author Manuscript

NIH-PA Author Manuscript

NIH-PA Author Manuscript

et al., 2005), this discrepancy suggests that the molecular signaling cascade described above operates with a lower induction threshold in the PAG compared to the spinal cord. Whether higher midbrain density of group I mGluRs, PLCβ, DGL-α or CB_1 (or all) underlies the enhanced sensitivity and the more pronounced involvement of PAG in SIA is an interesting question to examine in future experiments. It is also possible that the volume of rimonabant administered intrathecally to the lumbar enlargement was insufficient to overcome the impact of exposure to footshock stress at multiple segmental levels (i.e. multiple dermatomes are in contact with the grid floor that delivers footshock stress, including the forepaws and the rear paws)]. Opposing effects of rimonabant in blocking CB_1 receptors localized to both GABAergic and glutamatergic neurons could also result in changes in synaptic signaling that counteract each other and result in no net change in behavior. In any case, our studies collectively suggest that activation of group I mGluRs enhances endocannabinoid-mediated stress antinociception through the $mGluR_5$-DGL-2-AG pathway via CB_1 receptor activation at the spinal level.

Previous behavioral studies indicated that in several models of acute or chronic pain, pharmacological stimulation of group I mGluRs by intrathecal application of high doses of DHPG had pro-nociceptive effects (Fisher & Coderre, 1996a,b, 1998; Karim *et al.*, 2001; Adwanikar *et al.*, 2004; Gabra *et al.*, 2007). Conversely, specific blockade of $mGluR_5$ by MPEP applied at high concentrations induced analgesia (Karim *et al.*, 2001; Walker *et al.*, 2001; Fisher *et al.*, 2002) and blocked neuronal activity in the dorsal horn induced by noxious stimulation (Fisher & Coderre, 1996a). These observations are generally in accordance with the dendritic localization of postsynaptic $mGluR_5$ responding to glutamatergic nociceptive primary afferents, implying the involvement of $mGluR_5$ in the spinal processing of nociceptive information. However, in the present experiments, DHPG and MPEP were used at ten times lower concentrations which did not alter basal nociceptive thresholds in the tail-flick test *per se* and enhanced or reduced stress-induced analgesia, respectively, under conditions in which 2-AG is specifically mobilized at the spinal level. This dose difference suggests that activation of group I mGluRs may first have an antinociceptive effect by evoking 2-AG synthesis and release in given pain paradigms, whereas higher ratio of glutamatergic activation of nociceptive neurons may lead to the initation of other, predominantly pro-nociceptive signaling cascades.

In the paradigm of non-opioid stress-induced analgesia (Hohmann *et al.*, 2005) used in our experiments, the delivery of a three min continuous electric footshock is followed by the reduction of pain sensation measured by tail-flick latency, resulting in intersegmentally mediated endocannabinoid-dependent stress antinociception. A possible scenario is that primary afferent terminals of the hindleg, located in lumbar spinal segments (L2-L6, Swett & Woolf, 1985), releasing excessive glutamate following footshock, may trigger $mGluR_5$-DGL-α-mediated 2-AG production in second order neurons. Interneurons located in the area of tail afferent nociceptor terminals (S3-Co3, Grossman *et al.* 1982), and making propriospinal connections linking these nociceptors to tail-flick motoneurons in L4-Co2 segments (Grossman *et al.* 1982), might impinge on 2-AG-releasing interneurons. Thus, 2-AG may mediate homo- and/or heterosynaptic inhibition of nociception acting on presynaptic CB_1 located on hindleg afferent terminals or intersegmental interneuron axon endings, respectively. Both scenarios are supported by our electron microscopic observations.

Group I mGluR activation is involved in various forms of homo- and heterosynaptic plasticity (for review, see Bellone *et al.*, 2008), including induction of long-term depression (LTD) of synaptic transmission between Aδ-fibers and second order neurons (Heinke & Sandkuhler, 2005). Thus, a possible physiological mechanism of inhibition of spinal pain processing may be an $mGluR_5$-dependent, endocannabinoid-mediated short-term suppression or LTD of synaptic transmission, already described in the brain (Robbe *et al.*, 2002; Chevaleyre & Castillo, 2003; Uchigashima *et al.*, 2007).

NIH-PA Author Manuscript

NIH-PA Author Manuscript

NIH-PA Author Manuscript

The present study focused on understanding neuronal 2-AG signaling, because glial expression levels of DGL-α in naive animals remained under the detection threshold of our methods. However, in the spinal cord, potential non-neuronal sources of endocannabinoids should also be considered, particularly under conditions of injury or other pathological challenge. In experiments using cell cultures, glial cells such as astrocytes and microglia express $mGluR_5$ receptors (Biber *et al.*, 1999) and possess the capacity for 2-AG synthesis and release (Walter & Stella, 2003; Walter *et al.*, 2004; Carrier *et al.*, 2004; Witting *et al.*, 2004). At the supraspinal level, microglial cells are activated after footshock (Blandino *et al.*, 2006), suggesting that activated glial cells could also potentially participate in spinal 2-AG signaling. Further studies are thus needed to asses the relative contribution of glial endocannabinoids to antinociception in different pain paradigms.

Taken together, our findings in the spinal cord are consistent with a common molecular architecture responsible for retrograde 2-AG signaling throughout the brain, in which 2-AG may be a key negative feed-back signal at many central synapses (Katona & Freund, 2008). Based on the findings reported here, we propose that this retrograde signaling pathway also controls nociceptive responding *in vivo* by suppressing pain transmission at the spinal level in an activity-dependent manner.

Supplementary Material

Refer to Web version on PubMed Central for supplementary material.

Acknowledgments

This work was supported by Hungarian Health Science Council (ETT) Grant 561/2006 and the Janos Bolyai scholarship (I.K.), and by National Institutes of Health Grants DA021644, DA022478 and DA022702 (A.G.H.), DA11322 and DA21696 (K.M.). The authors are grateful to Dr. Anke Tappe-Theodore and Gabriella M. Urbán for their valuable contribution to preliminary experiments, to Barna Dudok and Dr. Mark D. Eyre for help with confocal microscopic analysis and to Prof. Tamás F. Freund for supporting this project. We also thank Profs Rohini Kuner, Hanns Ulrich Zeilhofer and Miklós Réthelyi for discussion and Dr. Viktor Varga for comments on the manuscript, and John Calhoun, Katalin Lengyel, Katalin Iványi, Emőke Szépné Simon and Győző Goda for excellent technical assistance.

Abbreviations

2-AG
: 2-arachidonoylglycerol

CB_1
: type 1 cannabinoid receptor

DAB
: 3,3′-diaminobenzidine

DGL-α
: diacylglycerol lipase-alpha

DHPG
: (*S*)-3,5-dihydroxyphenylglycine

$mGluR_5$
: metabotropic glutamate receptor 5

MPEP
: 2-methyl-6-(phenylethynyl)pyridine

NIH-PA Author Manuscript

NIH-PA Author Manuscript

NIH-PA Author Manuscript

SIA

stress-induced analgesia

THL

N-formyl-L-leucine (1S)-1-[[(2S,3S)-3-hexyl-4-oxo-2-oxetanyl]methyl] dodecyl ester ((−)-tetrahydrolipstatin

References

Adwanikar H, Karim F, Gereau RWt. Inflammation persistently enhances nocifensive behaviors mediated by spinal group I mGluRs through sustained ERK activation. Pain 2004;111:125–135. [PubMed: 15327816]

Agarwal N, Pacher P, Tegeder I, Amaya F, Constantin CE, Brenner GJ, Rubino T, Michalski CW, Marsicano G, Monory K, Mackie K, Marian C, Batkai S, Parolaro D, Fischer MJ, Reeh P, Kunos G, Kress M, Lutz B, Woolf CJ, Kuner R. Cannabinoids mediate analgesia largely via peripheral type 1 cannabinoid receptors in nociceptors. Nature Neuroscience 2007;10:870–879.

Ahluwalia J, Urban L, Capogna M, Bevan S, Nagy I. Cannabinoid 1 receptors are expressed in nociceptive primary sensory neurons. Neuroscience 2000;100:685–688. [PubMed: 11036202]

Alvarez FJ, Villalba RM, Carr PA, Grandes P, Somohano PM. Differential distribution of metabotropic glutamate receptors 1a, 1b, and 5 in the rat spinal cord. J Comp Neurol 2000;422:464–487. [PubMed: 10861520]

Bellone C, Luscher C, Mameli M. Mechanisms of synaptic depression triggered by metabotropic glutamate receptors. Cell Mol Life Sci 2008;65:2913–2923. [PubMed: 18712277]

Bisogno T, Howell F, Williams G, Minassi A, Cascio MG, Ligresti A, Matias I, Schiano-Moriello A, Paul P, Williams EJ, Gangadharan U, Hobbs C, Di Marzo V, Doherty P. Cloning of the first sn1-DAG lipases points to the spatial and temporal regulation of endocannabinoid signaling in the brain. Journal of Cell Biology 2003;163:463–468. [PubMed: 14610053]

Bisogno T, Cascio MG, Saha B, Mahadevan A, Urbani P, Minassi A, Appendino G, Saturnino C, Martin B, Razdan R, Di Marzo V. Development of the first potent and specific inhibitors of endocannabinoid biosynthesis. Biochim Biophys Acta 2006;1761:205–212. [PubMed: 16466961]

Biber K, Laurie DJ, Berthele A, Sommer B, Tolle TR, Gebicke-Harter PJ, van Calker D, Boddeke HW. Expression and signaling of group I metabotropic glutamate receptors in astrocytes and microglia. J Neurochem 1999;72:1671–1680. [PubMed: 10098876]

Blandino P Jr, Barnum CJ, Deak T. The involvement of norepinephrine and microglia in hypothalamic and splenic IL-1beta responses to stress. J Neuroimmunol 2006;173:87–95. [PubMed: 16386803]

Blankman JL, Simon GM, Cravatt BF. A comprehensive profile of brain enzymes that hydrolyze the endocannabinoid 2-arachidonoylglycerol. Chem Biol 2007;14:1347–1356. [PubMed: 18096503]

Carrier EJ, Kearn CS, Barkmeier AJ, Breese NM, Yang W, Nithipatikom K, Pfister SL, Campbell WB, Hillard CJ. Cultured rat microglial cells synthesize the endocannabinoid 2-arachidonylglycerol, which increases proliferation via a CB2 receptor-dependent mechanism. Mol Pharmacol 2004;65:999–1007. [PubMed: 15044630]

Chapman V. The cannabinoid CB1 receptor antagonist, SR141716A, selectively facilitates nociceptive responses of dorsal horn neurones in the rat. British Journal of Pharmacology 1999;127:1765–1767. [PubMed: 10482905]

Chevaleyre V, Castillo PE. Heterosynaptic LTD of hippocampal GABAergic synapses: a novel role of endocannabinoids in regulating excitability. Neuron 2003;38:461–472. [PubMed: 12741992]

D'Amour FE, Smith DL. A Method for Determining Loss of Pain Sensation. J Pharmacol Exp Ther 1941;72:74–79.

de Novellis V, Mariani L, Palazzo E, Vita D, Marabese I, Scafuro M, Rossi F, Maione S. Periaqueductal grey CB1 cannabinoid and metabotropic glutamate subtype 5 receptors modulate changes in rostral ventromedial medulla neuronal activities induced by subcutaneous formalin in the rat. Neuroscience 2005;134:269–281. [PubMed: 15953687]

Di Marzo V, Petrocellis LD. Plant, synthetic, and endogenous cannabinoids in medicine. Annual Review of Medicine 2006;57:553–574.

NIH-PA Author Manuscript

NIH-PA Author Manuscript

NIH-PA Author Manuscript

Dinh TP, Carpenter D, Leslie FM, Freund TF, Katona I, Sensi SL, Kathuria S, Piomelli D. Brain monoglyceride lipase participating in endocannabinoid inactivation. Proc Natl Acad Sci U S A 2002;99:10819–10824. [PubMed: 12136125]

Drew GM, Mitchell VA, Vaughan CW. Glutamate spillover modulates GABAergic synaptic transmission in the rat midbrain periaqueductal grey via metabotropic glutamate receptors and endocannabinoid signaling. Journal of Neuroscience 2008;28:808–815. [PubMed: 18216189]

Drew LJ, Harris J, Millns PJ, Kendall DA, Chapman V. Activation of spinal cannabinoid 1 receptors inhibits C-fibre driven hyperexcitable neuronal responses and increases [35S]GTPgammaS binding in the dorsal horn of the spinal cord of noninflamed and inflamed rats. European Journal of Neuroscience 2000;12:2079–2086. [PubMed: 10886347]

Egertova M, Elphick MR. Localisation of cannabinoid receptors in the rat brain using antibodies to the intracellular C-terminal tail of CB. Journal of Comparative Neurology 2000;422:159–171. [PubMed: 10842224]

Fang X, McMullan S, Lawson SN, Djouhri L. Electrophysiological differences between nociceptive and non-nociceptive dorsal root ganglion neurones in the rat in vivo. J Physiol 2005;565:927–943. [PubMed: 15831536]

Farquhar-Smith WP, Egertova M, Bradbury EJ, McMahon SB, Rice AS, Elphick MR. Cannabinoid CB (1) receptor expression in rat spinal cord. Molecular and Cellular Neurosciences 2000;15:510–521. [PubMed: 10860578]

Fisher K, Coderre TJ. Comparison of nociceptive effects produced by intrathecal administration of mGluR agonists. Neuroreport 1996a;7:2743–2747. [PubMed: 8981459]

Fisher K, Coderre TJ. The contribution of metabotropic glutamate receptors (mGluRs) to formalin-induced nociception. Pain 1996b;68:255–263. [PubMed: 9121812]

Fisher K, Coderre TJ. Hyperalgesia and allodynia induced by intrathecal (RS)-dihydroxyphenylglycine in rats. Neuroreport 1998;9:1169–1172. [PubMed: 9601688]

Fisher K, Lefebvre C, Coderre TJ. Antinociceptive effects following intrathecal pretreatment with selective metabotropic glutamate receptor compounds in a rat model of neuropathic pain. Pharmacol Biochem Behav 2002;73:411–418. [PubMed: 12117596]

Fritschy JM. Is my antibody-staining specific? How to deal with pitfalls of immunohistochemistry. European Journal of Neuroscience 2008;28:2365–2370. [PubMed: 19087167]

Fukudome Y, Ohno-Shosaku T, Matsui M, Omori Y, Fukaya M, Tsubokawa H, Taketo MM, Watanabe M, Manabe T, Kano M. Two distinct classes of muscarinic action on hippocampal inhibitory synapses: M2-mediated direct suppression and M1/M3-mediated indirect suppression through endocannabinoid signalling. European Journal of Neuroscience 2004;19:2682–2692. [PubMed: 15147302]

Gabra BH, Kessler FK, Ritter JK, Dewey WL, Smith FL. Decrease in N-methyl-D-aspartic acid receptor-NR2B subunit levels by intrathecal short-hairpin RNA blocks group I metabotropic glutamate receptor-mediated hyperalgesia. J Pharmacol Exp Ther 2007;322:186–194. [PubMed: 17405869]

Greenhouse SW, Geisser S. On methods in the analysis of profile data. Psychometrika 1959;24:95–112.

Guindon J, Hohmann AG. Cannabinoid CB2 receptors: a therapeutic target for the treatment of inflammatory and neuropathic pain. British Journal of Pharmacology 2008;153:319–334. [PubMed: 17994113]

Grossman ML, Basbaum AI, Fields HL. Afferent and efferent connections of the rat tail flick reflex (a model used to analyze pain control mechanisms). Journal of Comparative Neurology 1982;206:9–16. [PubMed: 7096630]

Hashimotodani Y, Ohno-Shosaku T, Kano M. Presynaptic monoacylglycerol lipase activity determines basal endocannabinoid tone and terminates retrograde endocannabinoid signaling in the hippocampus. Journal of Neuroscience 2007;27:1211–1219. [PubMed: 17267577]

Hashimotodani Y, Ohno-Shosaku T, Maejima T, Fukami K, Kano M. Pharmacological evidence for the involvement of diacylglycerol lipase in depolarization-induced endocanabinoid release. Neuropharmacology 2008;54:58–67. [PubMed: 17655882]

Heinke B, Sandkuhler J. Signal transduction pathways of group I metabotropic glutamate receptor-induced long-term depression at sensory spinal synapses. Pain 2005;118:145–154. [PubMed: 16185811]

NIH-PA Author Manuscript

NIH-PA Author Manuscript

NIH-PA Author Manuscript

Hohmann AG, Herkenham M. Regulation of cannabinoid and mu opioid receptors in rat lumbar spinal cord following neonatal capsaicin treatment. Neuroscience Letters 1998;252:13–16. [PubMed: 9756347]

Hohmann AG, Tsou K, Walker JM. Cannabinoid modulation of wide dynamic range neurons in the lumbar dorsal horn of the rat by spinally administered WIN55,212–2. Neuroscience Letters 1998;257:119–122. [PubMed: 9870334]

Hohmann AG, Herkenham M. Localization of central cannabinoid CB1 receptor messenger RNA in neuronal subpopulations of rat dorsal root ganglia: a double-label in situ hybridization study. Neuroscience 1999;90:923–931. [PubMed: 10218792]

Hohmann AG, Suplita RL 2nd. Endocannabinoid mechanisms of pain modulation. The AAPS Journal 2006;8:E693–708. [PubMed: 17233533]

Hohmann AG, Briley EM, Herkenham M. Pre- and postsynaptic distribution of cannabinoid and mu opioid receptors in rat spinal cord. Brain Research 1999;822:17–25. [PubMed: 10082879]

Hohmann AG, Suplita RL, Bolton NM, Neely MH, Fegley D, Mangieri R, Krey JF, Walker JM, Holmes PV, Crystal JD, Duranti A, Tontini A, Mor M, Tarzia G, Piomelli D. An endocannabinoid mechanism for stress-induced analgesia. Nature 2005;435:1108–1112. [PubMed: 15973410]

Jung KM, Astarita G, Zhu C, Wallace M, Mackie K, Piomelli D. A key role for diacylglycerol lipase-alpha in metabotropic glutamate receptor-dependent endocannabinoid mobilization. Molecular Pharmacology 2007;72:612–621. [PubMed: 17584991]

Jung KM, Mangieri R, Stapleton C, Kim J, Fegley D, Wallace M, Mackie K, Piomelli D. Stimulation of endocannabinoid formation in brain slice cultures through activation of group I metabotropic glutamate receptors. Molecular Pharmacology 2005;68:1196–1202. [PubMed: 16051747]

Karim F, Wang CC, Gereau RWt. Metabotropic glutamate receptor subtypes 1 and 5 are activators of extracellular signal-regulated kinase signaling required for inflammatory pain in mice. J Neurosci 2001;21:3771–3779. [PubMed: 11356865]

Katona I, Freund TF. Endocannabinoid signaling as a synaptic circuit breaker in neurological disease. Nature Medicine 2008;14:923–930.

Katona I, Sperlagh B, Sik A, Kafalvi A, Vizi ES, Mackie K, Freund TF. Presynaptically located CB1 cannabinoid receptors regulate GABA release from axon terminals of specific hippocampal interneurons. Journal of Neuroscience 1999;19:4544–4558. [PubMed: 10341254]

Katona I, Urban GM, Wallace M, Ledent C, Jung KM, Piomelli D, Mackie K, Freund TF. Molecular composition of the endocannabinoid system at glutamatergic synapses. Journal of Neuroscience 2006;26:5628–5637. [PubMed: 16723519]

Kawamura Y, Fukaya M, Maejima T, Yoshida T, Miura E, Watanabe M, Ohno-Shosaku T, Kano M. The CB1 cannabinoid receptor is the major cannabinoid receptor at excitatory presynaptic sites in the hippocampus and cerebellum. Journal of Neuroscience 2006;26:2991–3001. [PubMed: 16540577]

Kelly S, Chapman V. Selective cannabinoid CB1 receptor activation inhibits spinal nociceptive transmission in vivo. Journal of Neurophysiology 2001;86:3061–3064. [PubMed: 11731561]

Kogan NM, Mechoulam R. Cannabinoids in health and disease. Dialogues in Clinical Neuroscience 2007;9:413–430. [PubMed: 18286801]

Lafourcade M, Elezgarai I, Mato S, Bakiri Y, Grandes P, Manzoni OJ. Molecular components and functions of the endocannabinoid system in mouse prefrontal cortex. PLoS ONE 2007;2:e709. [PubMed: 17684555]

Ledent C, Valverde O, Cossu G, Petitet F, Aubert JF, Beslot F, Bohme GA, Imperato A, Pedrazzini T, Roques BP, Vassart G, Fratta W, Parmentier M. Unresponsiveness to cannabinoids and reduced addictive effects of opiates in CB1 receptor knockout mice. Science 1999;283:401–404. [PubMed: 9888857]

Lujan R, Nusser Z, Roberts JD, Shigemoto R, Somogyi P. Perisynaptic location of metabotropic glutamate receptors mGluR1 and mGluR5 on dendrites and dendritic spines in the rat hippocampus. European Journal of Neuroscience 1996;8:1488–1500. [PubMed: 8758956]

Maejima T, Hashimoto K, Yoshida T, Aiba A, Kano M. Presynaptic inhibition caused by retrograde signal from metabotropic glutamate to cannabinoid receptors. Neuron 2001;31:463–475. [PubMed: 11516402]

NIH-PA Author Manuscript

NIH-PA Author Manuscript

NIH-PA Author Manuscript

Makara JK, Mor M, Fegley D, Szabo SI, Kathuria S, Astarita G, Duranti A, Tontini A, Tarzia G, Rivara S, Freund TF, Piomelli D. Selective inhibition of 2-AG hydrolysis enhances endocannabinoid signaling in hippocampus. Nature Neuroscience 2005;8:1139–1141.

Matyas F, Urban GM, Watanabe M, Mackie K, Zimmer A, Freund TF, Katona I. Identification of the sites of 2-arachidonoylglycerol synthesis and action imply retrograde endocannabinoid signaling at both GABAergic and glutamatergic synapses in the ventral tegmental area. Neuropharmacology 2008;54:95–107. [PubMed: 17655884]

Mechoulam R, Ben-Shabat S, Hanus L, Ligumsky M, Kaminski NE, Schatz AR, Gopher A, Almog S, Martin BR, Compton DR, et al. Identification of an endogenous 2-monoglyceride, present in canine gut, that binds to cannabinoid receptors. Biochemical Pharmacology 1995;50:83–90. [PubMed: 7605349]

Melis M, Perra S, Muntoni AL, Pillolla G, Lutz B, Marsicano G, Di Marzo V, Gessa GL, Pistis M. Prefrontal cortex stimulation induces 2-arachidonoyl-glycerol-mediated suppression of excitation in dopamine neurons. Journal of Neuroscience 2004;24:10707–10715. [PubMed: 15564588]

Millan MJ. The induction of pain: an integrative review. Progress in Neurobiology 1999;57:1–164. [PubMed: 9987804]

Mitrirattanakul S, Ramakul N, Guerrero AV, Matsuka Y, Ono T, Iwase H, Mackie K, Faull KF, Spigelman I. Site-specific increases in peripheral cannabinoid receptors and their endogenous ligands in a model of neuropathic pain. Pain 2006;126:102–114. [PubMed: 16844297]

Morisset V, Urban L. Cannabinoid-induced presynaptic inhibition of glutamatergic EPSCs in substantia gelatinosa neurons of the rat spinal cord. Journal of Neurophysiology 2001;86:40–48. [PubMed: 11431486]

Pacher P, Batkai S, Kunos G. The endocannabinoid system as an emerging target of pharmacotherapy. Pharmacological Reviews 2006;58:389–462. [PubMed: 16968947]

Palazzo E, Marabese I, de Novellis V, Oliva P, Rossi F, Berrino L, Maione S. Metabotropic and NMDA glutamate receptors participate in the cannabinoid-induced antinociception. Neuropharmacology 2001;40:319–326. [PubMed: 11166324]

Pertwee RG. Cannabinoid receptors and pain. Progress in Neurobiology 2001;63:569–611. [PubMed: 11164622]

Petrosino S, Palazzo E, de Novellis V, Bisogno T, Rossi F, Maione S, Di Marzo V. Changes in spinal and supraspinal endocannabinoid levels in neuropathic rats. Neuropharmacology 2007;52:415–422. [PubMed: 17011598]

Pin JP, Duvoisin R. The metabotropic glutamate receptors: structure and functions. Neuropharmacology 1995;34:1–26. [PubMed: 7623957]

Piomelli D. The molecular logic of endocannabinoid signalling. Nature Reviews Neuroscience 2003;4:873–884.

Pitcher MH, Ribeiro-da-Silva A, Coderre TJ. Effects of inflammation on the ultrastructural localization of spinal cord dorsal horn group I metabotropic glutamate receptors. Journal of Comparative Neurology 2007;505:412–423. [PubMed: 17912745]

Price TJ, Helesic G, Parghi D, Hargreaves KM, Flores CM. The neuronal distribution of cannabinoid receptor type 1 in the trigeminal ganglion of the rat. Neuroscience 2003;120:155–162. [PubMed: 12849749]

Racz I, Nadal X, Alferink J, Banos JE, Rehnelt J, Martin M, Pintado B, Gutierrez-Adan A, Sanguino E, Manzanares J, Zimmer A, Maldonado R. Crucial role of CB(2) cannabinoid receptor in the regulation of central immune responses during neuropathic pain. Journal of Neuroscience 2008;28:12125–12135. [PubMed: 19005077]

Réthelyi M, Light AR, Perl ER. Synaptic complexes formed by functionally defined primary afferent units with fine myelinated fibers. Journal of Comparative Neurology 1982;207:381–393. [PubMed: 6288776]

Ribeiro-da-Silva A, Coimbra A. Two types of synaptic glomeruli and their distribution in laminae I–III of the rat spinal cord. Journal of Comparative Neurology 1982;209:176–186. [PubMed: 6890076]

Ribeiro-da-Silva, A. Substantia Gelatinosa of Spinal Cord. In: Paxinos, G., editor. The Rat Nervous System 2nd Edition. Academic Press; 1995. p. 47-59.

NIH-PA Author Manuscript

NIH-PA Author Manuscript

NIH-PA Author Manuscript

Robbe D, Kopf M, Remaury A, Bockaert J, Manzoni OJ. Endogenous cannabinoids mediate long-term synaptic depression in the nucleus accumbens. Proceedings of the National Academy of Sciences of the United States of America 2002;99:8384–8388. [PubMed: 12060781]

Salio C, Fischer J, Franzoni MF, Conrath M. Pre- and postsynaptic localizations of the CB1 cannabinoid receptor in the dorsal horn of the rat spinal cord. Neuroscience 2002;110:755–764. [PubMed: 11934482]

Strangman NM, Walker JM. Cannabinoid WIN 55,212-2 inhibits the activity-dependent facilitation of spinal nociceptive responses. Journal of Neurophysiology 1999;82:472–477. [PubMed: 10400973]

Sugiura T, Kishimoto S, Oka S, Gokoh M. Biochemistry, pharmacology and physiology of 2-arachidonoylglycerol, an endogenous cannabinoid receptor ligand. Progress in Lipid Research 2006;45:405–446. [PubMed: 16678907]

Sugiura T, Kondo S, Sukagawa A, Nakane S, Shinoda A, Itoh K, Yamashita A, Waku K. 2-Arachidonoylglycerol: a possible endogenous cannabinoid receptor ligand in brain. Biochemical and Biophysical Research Communications 1995;215:89–97. [PubMed: 7575630]

Suplita RL 2nd, Farthing JN, Gutierrez T, Hohmann AG. Inhibition of fatty-acid amide hydrolase enhances cannabinoid stress-induced analgesia: sites of action in the dorsolateral periaqueductal gray and rostral ventromedial medulla. Neuropharmacology 2005;49:1201–1209. [PubMed: 16129456]

Suplita RL 2nd, Gutierrez T, Fegley D, Piomelli D, Hohmann AG. Endocannabinoids at the spinal level regulate, but do not mediate, nonopioid stress-induced analgesia. Neuropharmacology 2006;50:372–379. [PubMed: 16316669]

Suplita RL 2nd, Eisenstein SA, Neely MH, Moise AM, Hohmann AG. Cross-sensitization and cross-tolerance between exogenous cannabinoid antinociception and endocannabinoid-mediated stress-induced analgesia. Neuropharmacology 2008;54:161–171. [PubMed: 17714742]

Swett JE, Woolf CJ. The somatotopic organization of primary afferent terminals in the superficial laminae of the dorsal horn of the rat spinal cord. Journal of Comparative Neurology 1985;231:66–77. [PubMed: 3968229]

Tao YX, Li YQ, Zhao ZQ, Johns RA. Synaptic relationship of the neurons containing a metabotropic glutamate receptor, MGluR5, with nociceptive primary afferent and GABAergic terminals in rat spinal superficial laminae. Brain Research 2000;875:138–143. [PubMed: 10967307]

Uchigashima M, Narushima M, Fukaya M, Katona I, Kano M, Watanabe M. Subcellular arrangement of molecules for 2-arachidonoyl-glycerol-mediated retrograde signaling and its physiological contribution to synaptic modulation in the striatum. Journal of Neuroscience 2007;27:3663–3676. [PubMed: 17409230]

Yaksh TL, Rudy TA. Chronic catheterization of the spinal subarachnoid space. Physiology & Behavior 1976;17:1031–1036. [PubMed: 14677603]

Yoshida T, Fukaya M, Uchigashima M, Miura E, Kamiya H, Kano M, Watanabe M. Localization of diacylglycerol lipase-alpha around postsynaptic spine suggests close proximity between production site of an endocannabinoid, 2-arachidonoyl-glycerol, and presynaptic cannabinoid CB1 receptor. Journal of Neuroscience 2006;26:4740–4751. [PubMed: 16672646]

Walker K, Bowes M, Panesar M, Davis A, Gentry C, Kesingland A, Gasparini F, Spooren W, Stoehr N, Pagano A, Flor PJ, Vranesic I, Lingenhoehl K, Johnson EC, Varney M, Urban L, Kuhn R. Metabotropic glutamate receptor subtype 5 (mGlu5) and nociceptive function. I. Selective blockade of mGlu5 receptors in models of acute, persistent and chronic pain. Neuropharmacology 2001;40:1–9. [PubMed: 11077065]

Walker JM, Hohmann AG. Cannabinoid mechanisms of pain suppression. Handb Exp Pharmacol 2005:509–554. [PubMed: 16596786]

Walter L, Dinh T, Stella N. ATP induces a rapid and pronounced increase in 2-arachidonoylglycerol production by astrocytes, a response limited by monoacylglycerol lipase. J Neurosci 2004;24:8068–8074. [PubMed: 15371507]

Walter L, Stella N. Endothelin-1 increases 2-arachidonoyl glycerol (2-AG) production in astrocytes. Glia 2003;44:85–90. [PubMed: 12951660]

Witting A, Walter L, Wacker J, Moller T, Stella N. P2X7 receptors control 2-arachidonoylglycerol production by microglial cells. Proc Natl Acad Sci U S A 2004;101:3214–3219. [PubMed: 14976257]

Zimmer A, Zimmer AM, Hohmann AG, Herkenham M, Bonner TI. Increased mortality, hypoactivity, and hypoalgesia in cannabinoid CB1 receptor knockout mice. Proceedings of the National Academy of Sciences of the United States of America 1999;96:5780–5785. [PubMed: 10318961]

Zimmermann M. Ethical guidelines for investigations of experimental pain in conscious animals. Pain 1983;16:109–110. [PubMed: 6877845]

NIH-PA Author Manuscript

NIH-PA Author Manuscript

NIH-PA Author Manuscript

NIH-PA Author Manuscript
NIH-PA Author Manuscript
NIH-PA Author Manuscript

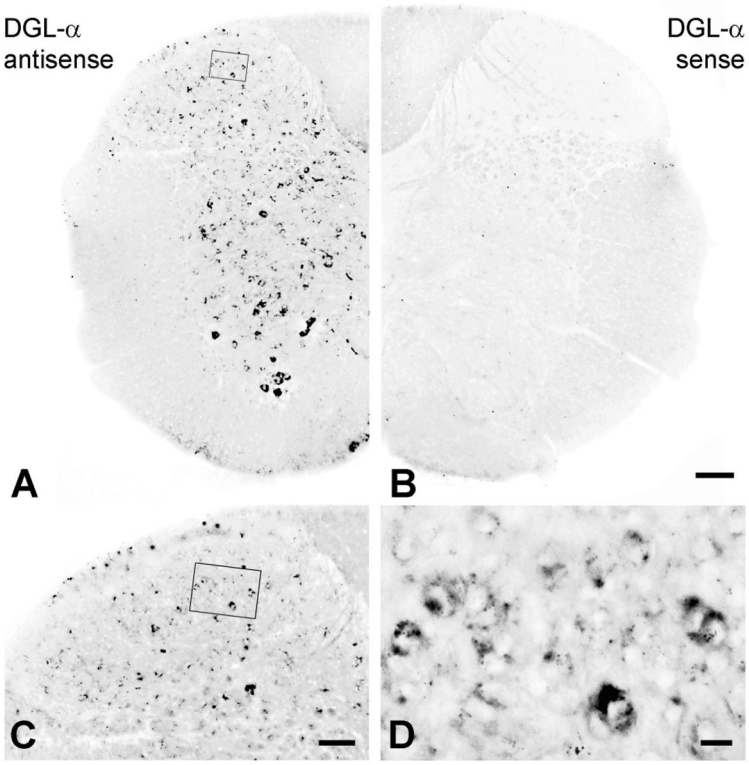

Figure 1. Dorsal horn neurons express high levels of DGL-α mRNA

(A) *In situ* hybridization using an antisense riboprobe for DGL-α reveals the widespread distribution of neurons in the mouse spinal cord that exhibit high levels of DGL-α mRNA. (B) In contrast, staining reaction with the sense probe directed against the complementary mRNA sequence shows no labeling, demonstrating the specificity of the *in situ* hybridization. (C, D) DGL-α-expressing cells in the dorsal horn of the spinal cord at higher magnification. (Boxed area in A and C is enlarged in D.) Note, that DGL-α mRNA levels vary from low to high in distinct cells (D), though no obvious layer-specific pattern is observable in relation to expression levels (C). Scale bars: A–B, 100 μm; C, 50 μm; D, 10 μm.

NIH-PA Author Manuscript

NIH-PA Author Manuscript

NIH-PA Author Manuscript

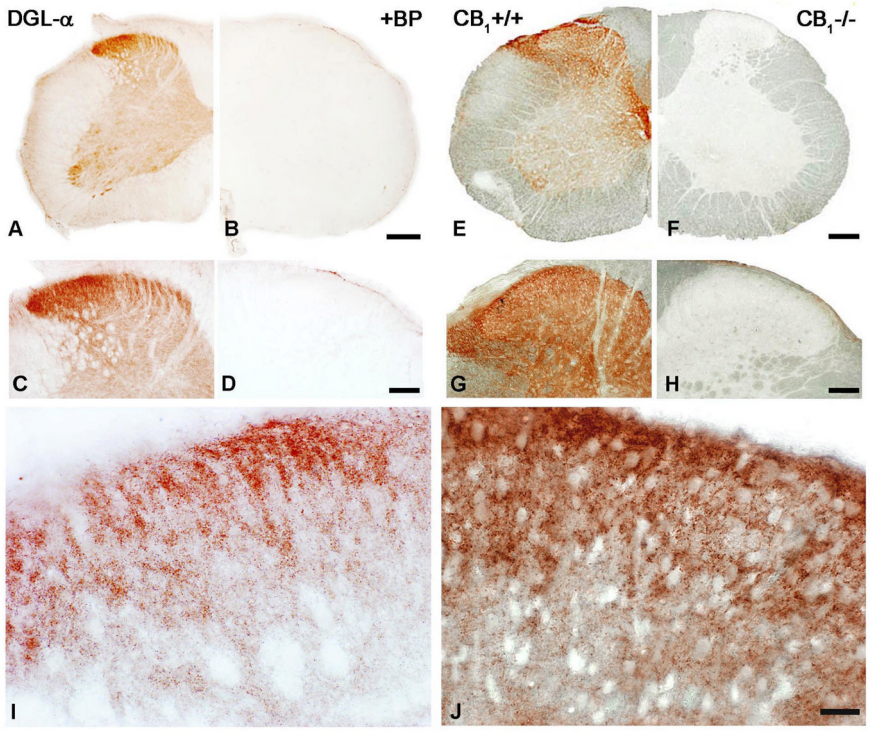

Figure 2. Accumulation of DGL-α and CB_1 cannabinoid receptor proteins in the dorsal horn of mouse spinal cord

(A,C) Light micrographs of DGL-α-immunoreactivity in the spinal cord using the 'INT' antibody. The highest density of immunostaining is located in the superficial layers. In addition, a number of immunopositive cell bodies are visualized in the ventral horn. (B,D) The specificity of the antibody is indicated by the lack of immunostaining in the presence of its blocking peptide. (E,G) Immunostaining for CB_1 receptors in the spinal cord of a wild-type (WT) mouse reveals the strongest labeling in the dorsal horn. High density of immunoreactivity is visible in the superficial layers of the spinal dorsal horn and in lamina X, around the central canal, which are the termination zones of somatic and visceral nociceptive axons, respectively. Immunostaining in ventral horn appears to be modest, except for lamina IX. (F,H) The specificity of the antibody is confirmed by the lack of immunostaining in a section from a CB_1-knockout animal. (I,J) At higher magnification, a very dense punctate staining pattern is observed in both the DGL-α- (I) and the CB_1- (J) immunostainings in the superficial layers, indicating the accumulation of these two proteins into selected subcellular compartments. Scale bars: A–B and E–F, 200 μm; C–D and G–H, 100 μm; I–J, 20 μm.

NIH-PA Author Manuscript
NIH-PA Author Manuscript
NIH-PA Author Manuscript

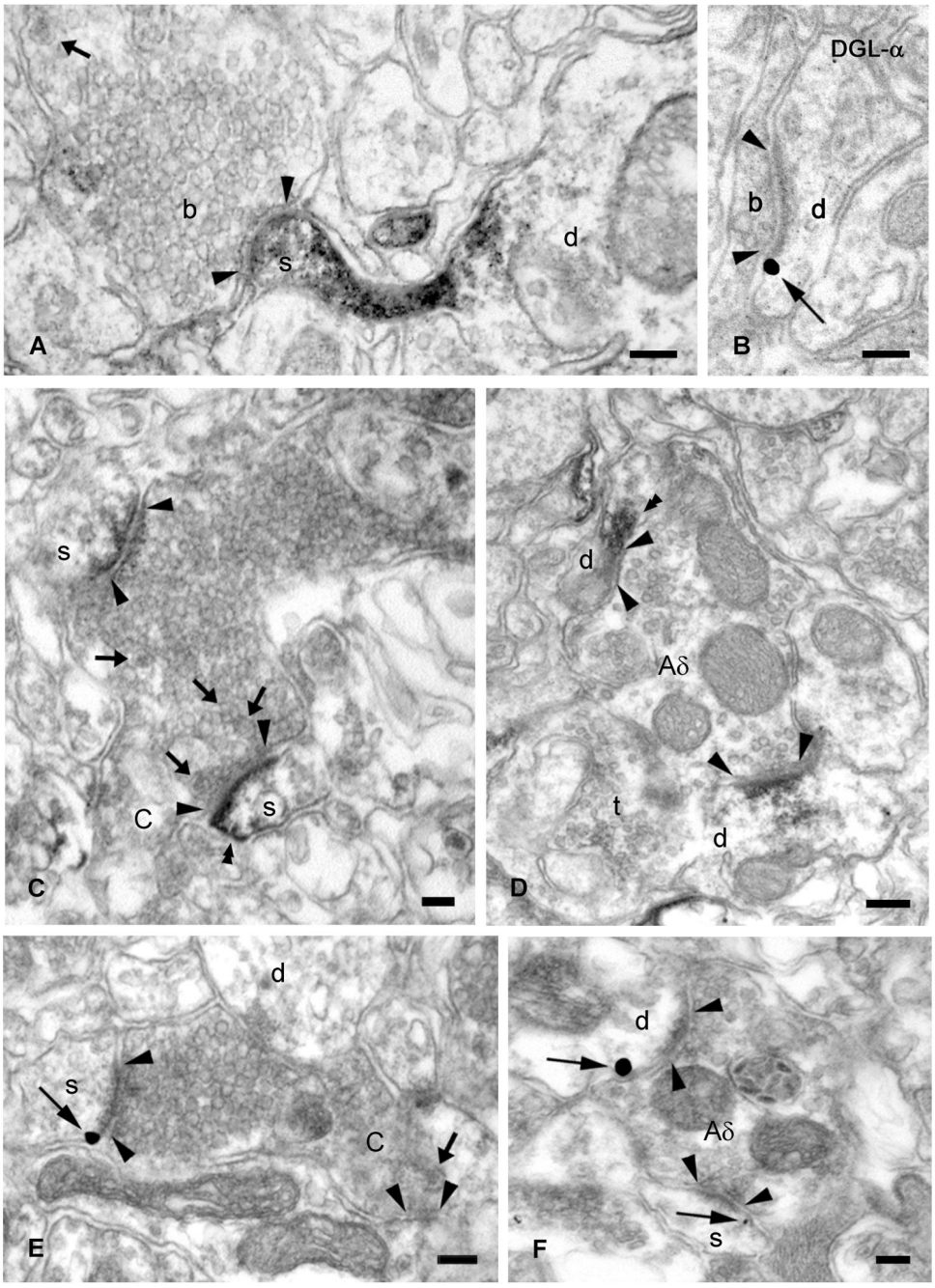

Figure 3. DGL-α is present in dendritic shafts and spine heads found postsynaptically to primary nociceptive terminals in the mouse superficial dorsal horn

(A,C,D) High-power electron micrographs of DGL-α immunostaining demonstrates that DGL-α is located postsynaptically, in the heads of dendritic spines (s) and in dendritic shafts (d) represented by the dense end product of the immunoperoxidase reaction (DAB) (double arrowheads). These DGL-α-containing spines and shafts receive asymmetrical synapses (arrowheads) from DGL-α-negative peptidergic nonglomerular boutons (A), type I synaptic glomeruli (C-nociceptive terminal in C) or type II synaptic glomeruli (Aδ-nociceptive terminal in D). Note the small, indented type I central terminal with dark axoplasm, closely packed spherical vesicles of variable size, lack of mitochondria, and several neuropeptide-containing

NIH-PA Author Manuscript

NIH-PA Author Manuscript

NIH-PA Author Manuscript

dense core vesicles (arrows) (C) and electron-lucent, larger type II bouton with regular contour, loosely distributed synaptic vesicles of uniform diameter, numerous mitochondria and axon endings (t) in apposition to the central terminal (D). (B,E,F) Pre-embedding immunogold staining demonstrates the presence of DGL-α on the plasma membrane of the head of dendritic spines and shafts. High-power electron micrographs show dendritic shafts (d) and spines (s) situated postsynaptically to small boutons (b in B) and central terminals of type I (in E) and type II synaptic glomeruli (in F), corresponding to C- and Aδ-nociceptive glutamatergic axon terminals, respectively. The gold particles (thin arrows), representing the precise subcellular localization of DGL-α, are always attached to the intracellular surface of the plasma membrane in accordance with the predicted position of the epitopes of DGL-α protein. Synaptic specializations are labeled with arrowheads, thick arrows depict dense core vesicles. Scale bars: A–E, 0.1 μm.

NIH-PA Author Manuscript
NIH-PA Author Manuscript
NIH-PA Author Manuscript

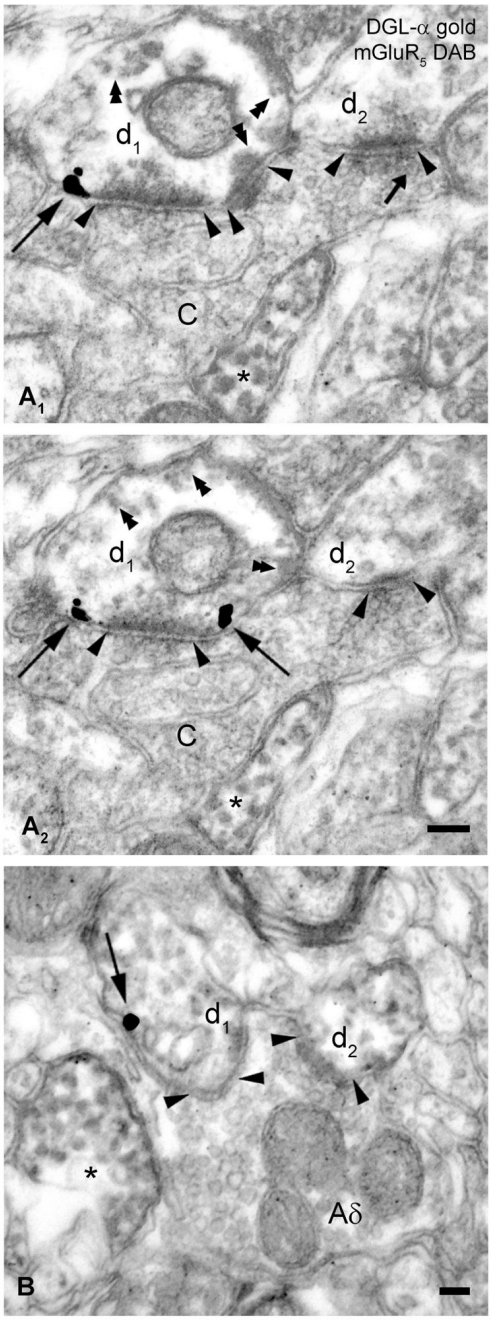

Figure 4. DGL-α co-localizes with mGluR$_5$ postsynaptically to primary nociceptive axon terminals

(A_1–B) Electron microscopic analysis of pre-embedding immunogold labeling of DGL-α combined with immunoperoxidase staining for mGluR$_5$ in the superficial layers of spinal dorsal horn of the mouse. (A_1–A_2) Serial high-resolution electron micrographs show that silver-intensified immunogold particles labeling DGL-α (indicated by long arrows) are located perisynaptically, on the plasma membrane of an mGluR$_5$-immunopositive dendrite (d_1) (represented by the diffusible immunoreaction end product DAB, indicated by double arrowheads). This dendrite is situated postsynaptically to a type I synaptic glomerulus (central axon terminal of a nociceptive C-fiber, labeled with C) forming several asymmetrical synapses (arrowheads). An asterisk labels another mGluR$_5$-positive dendritic profile. The small arrow

NIH-PA Author Manuscript

NIH-PA Author Manuscript

NIH-PA Author Manuscript

points to a dense core vesicle. (B) DGL-α and $mGluR_5$, represented by gold particle (arrow) and by DAB precipitate, respectively, are present in the same dendrite (d_1) receiving an asymmetrical, excitatory synapse (depicted by arrowheads) from a type II synaptic glomerulus (central Aδ-fiber terminal, labeled with Aδ), which makes a second synaptic contact with another $mGluR_5$-immunoreactive dendritic shaft (d_2). Asterisk labels a third, neighboring $mGluR_5$- positive dendrite. Note that the unusual faint color of the DAB precipitate is due to the conversely applied double immunostaining procedure (immunoperoxidase reaction was followed by pre-embedding immunogold staining). Scale bars: A–B, 0.1 μm.

NIH-PA Author Manuscript
NIH-PA Author Manuscript
NIH-PA Author Manuscript

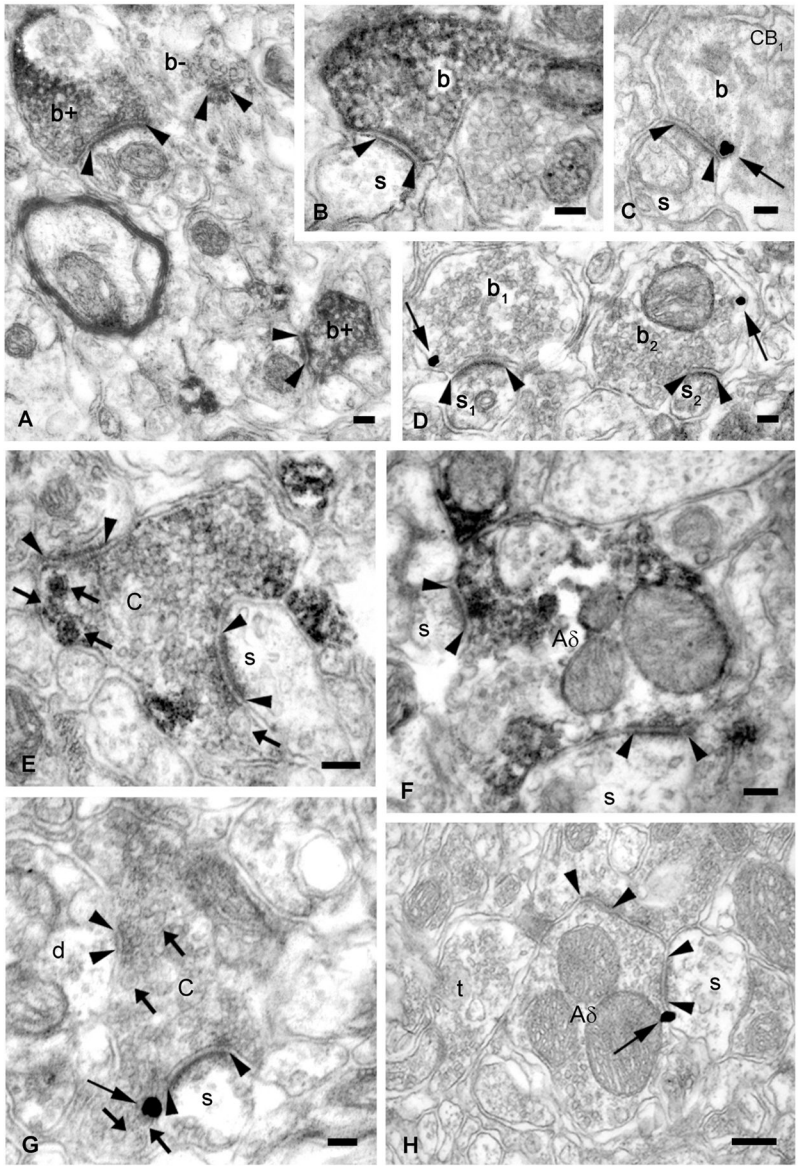

Figure 5. CB_1 receptors are located presynaptically on excitatory axon terminals in the mouse superficial dorsal horn

(A,B,E,F) High-power electron micrographs demonstrate that CB_1 receptors (visualized by DAB precipitate) are present in excitatory axon terminals forming asymmetric synapses (arrowheads), in the mouse dorsal spinal cord. Small boutons (b+ and b, in A and B) and synaptic glomeruli, corresponding to peptidergic C- (in E, dense core vesicles are indicated by arrows) and Aδ-fiber (in F) terminals, show strong CB_1 immunoreactivity. 'b-' in A labels an immunonegative axon ending. (C,D,G,H) Pre-embedding immunogold labeling for CB_1 demonstrates that the receptor (arrow) is located presynaptically on the plasma membrane of small excitatory terminals (b, b_1 and b_2, in C and D) and nociceptive C- or Aδ-boutons (in G or H, respectively). Dendritic spines in synaptic connection with small boutons and glomerular terminals, and a dendrite and an axon terminal surrounding the glomerular terminals are labeled by 's', 's_1', 's_2', 'd' and 't', respectively. Scale bars: A–B, 0.1 μm.

NIH-PA Author Manuscript

NIH-PA Author Manuscript

NIH-PA Author Manuscript

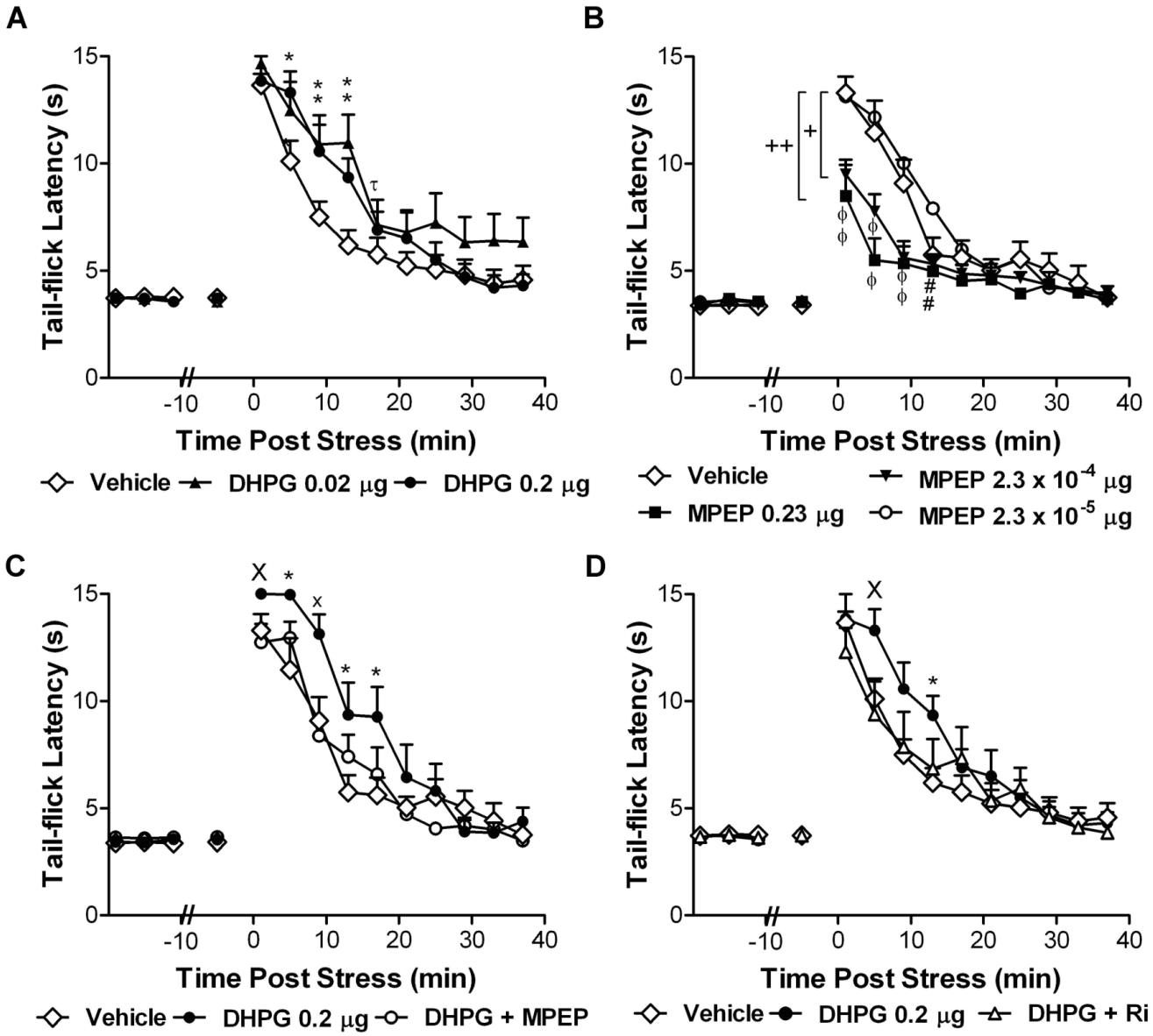

Figure 6. Activation of group I mGluR$_5$ receptors at the spinal level enhances stress antinociception through a CB$_1$-dependent mechanism

(A) The group I mGluR agonist DHPG (0.02 or 0.2 μg i.t.) produces a time-dependent enhancement of post-shock tail-flick latencies relative to vehicle treatment. (B) The mGluR$_5$ antagonist MPEP (2.3×10^{-4} μg and 0.23 μg i.t.) suppresses stress antinociception relative to control. A low concentration of MPEP (2.3×10^{-5} μg i.t.) alone does not alter stress antinociception. $+P < 0.05$ middle dose MPEP versus low dose MPEP, $++ P < 0.05$ high dose MPEP versus control and low dose MPEP (ANOVA, Fisher's PLSD *post hoc* test applied to main effects). (C) MPEP (2.3×10^{-5} μg i.t.) and (D) the CB$_1$ antagonist rimonabant (10 μg i.t.) block the time-dependent enhancement of stress antinociception induced by DHPG (0.2 μg i.t.). Data are mean ± SEM. In A–D: $^{*}P < 0.05$ versus control, $^{x}P < 0.05$ versus all groups, $^{X}P < 0.05$ versus antagonist pretreatment group, $^{\#}P < 0.05$ versus low dose, $^{\theta}P < 0.05$ versus control and low dose, $^{\tau}P < 0.05$ low dose versus control (ANOVA, Greenhouse-Geisser correction applied to interaction term of all repeated factors; N = 8–12 animals per group).

NIH-PA Author Manuscript

NIH-PA Author Manuscript

NIH-PA Author Manuscript

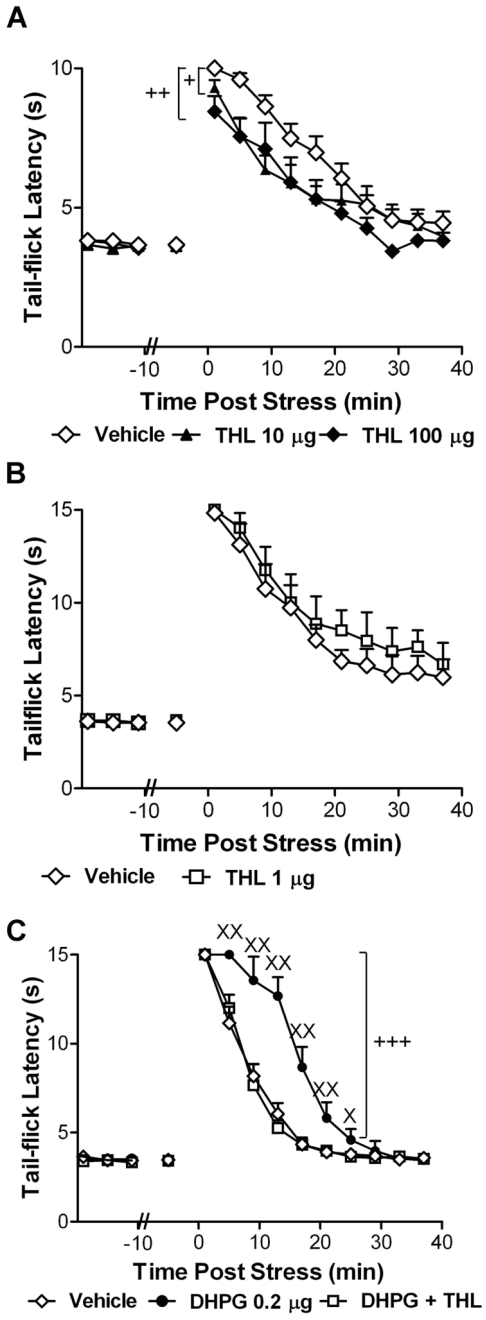

Figure 7. Activation of group I mGluRs at the spinal level enhances endocannabinoid-mediated stress antinociception through activation of diacylglycerol lipase (DGL)

(A) The DGL inhibitor THL (10 or 100 μg i.t.) suppresses post-shock tail-flick latencies relative to vehicle controls. $+P < 0.05$ THL (10 μg i.t.) versus control, $++P < 0.05$ THL (100 μg i.t.) versus control (ANOVA, Fisher's PLSD post hoc test applied to main effects; n = 6–15 animals per group). (B) THL (1 μg i.t.) does not alter stress antinociception. (C) The enhancement of endocannabinoid-mediated stress antinociception induced by DHPG (0.2 μg i.t.) was blocked by THL (1 μg i.t.). Data are mean ± SEM $+++P < 0.001$ DHPG versus all comparisons (ANOVA, Fisher's PLSD *post hoc* test applied to main effects), $^{XX}P < 0.01$, $^{X}P < 0.05$ versus

all groups (ANOVA, Greenhouse-Geisser correction applied to interaction term of all repeated factors; N = 8 per group).

NIH-PA Author Manuscript
NIH-PA Author Manuscript
NIH-PA Author Manuscript